AD-A168 900 INCREMENTAL QUENCH RESEARCH(U) TEXAS INSTRUMENTS INC 1/1
DALLAS L COLOMBO ET AL. 30 MAY 86 TI-U1-134375-F
ARO-22602.1-MS-A DAAG29-85-C-0005

UNCLASSIFIED F/G 20/2 NL

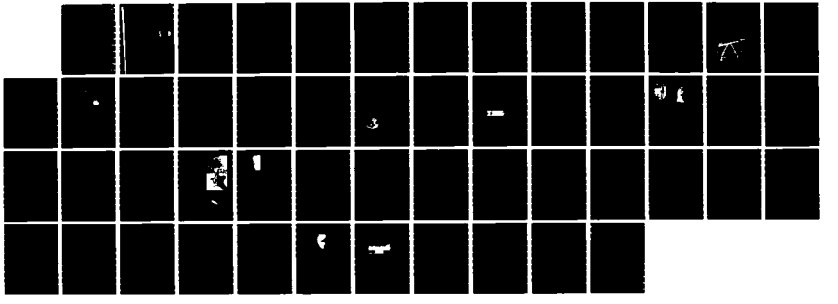

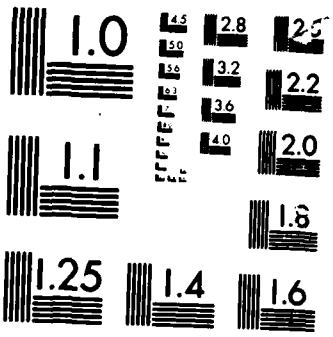

MICROCOPY CHART

INCREMENTAL QUENCH RESEARCH

Final Technical Report
Luigi Colombo
A.J. Syllaios

30 May 1986

Approved for public release.
Distribution unlimited.

Prepared for:

U.S. ARMY RESEARCH OFFICE
Research Triangle Park, North Carolina

Prepared by:

Texas Instruments Incorporated
Dallas, Texas

The view, opinions, and/or findings contained in this report are those of the author(s) and should not be construed as an official Department of the Army position, policy, or decision, unless so designated by other documentation.

UNCLASSIFIED

SECURITY CLASSIFICATION OF THIS PAGE (When Data Entered)

REPORT DOCUMENTATION PAGE		READ INSTRUCTIONS BEFORE COMPLETING FORM
1. REPORT NUMBER ARO 22602.1-MS-A	2. GOVT ACCESSION NO. N/A	3. RECIPIENT'S CATALOG NUMBER N/A
4. TITLE (and Subtitle) Incremental Quench Research		5. TYPE OF REPORT & PERIOD COVERED Final Technical Report 1 Nov 1984–31 Jan 1986
		6. PERFORMING ORG. REPORT NUMBER U1-134375-F
7. AUTHOR(s) L. Colombo, A.J. Syllaios		8. CONTRACT OR GRANT NUMBER(s) DAAG29-85-C-0005
9. PERFORMING ORGANIZATION NAME AND ADDRESS Texas Instruments Incorporated P.O. Box 660246, M/S 3137 Dallas, TX 75266		10. PROGRAM ELEMENT, PROJECT, TASK AREA & WORK UNIT NUMBERS
11. CONTROLLING OFFICE NAME AND ADDRESS U.S. Army Research Office P.O. Box 12211 Research Triangle Park, NC 27709		12. REPORT DATE 30 May 1986 13. NUMBER OF PAGES 44
14. MONITORING AGENCY NAME & ADDRESS(if different from Controlling Office)		15. SECURITY CLASS. (of this report) Unclassified 15a. DECLASSIFICATION/DOWNGRADING SCHEDULE

16. DISTRIBUTION STATEMENT (of this Report)

Approved for public release; distribution unlimited.

17. DISTRIBUTION STATEMENT (of the abstract entered in Block 20, if different from Report)

NA

18. SUPPLEMENTARY NOTES

The view, opinions, and/or findings contained in this report are those of the author(s) and should not be construed as an official Department of the Army position, policy, or decision, unless so designated by other documentation.

19. KEY WORDS (Continue on reverse side if necessary and identify by block number)

Mercury cadmium telluride
Incremental quenching
Traveling heater method

20. ABSTRACT (Continue on reverse side if necessary and identify by block number)

The growth of large homogeneous (Hg,Cd)Te single crystals by the incremental quenching process/traveling heater method was investigated. The method is based on the sequential freezing of shallow melts that have large surface-to-volume ratios onto a large diameter growing ingot. The resulting polycrystalline (Hg,Cd)Te ingot has a bimodal microstructure with small grains on the outer surface and dendrites at the center of the ingot. Subsequent annealing of the ingots at a temperature below the solidus promotes grain growth on the order of 25 mm in diameter. Growth of large area crystals by the traveling heater method has been successfully demonstrated where 22- by 40-mm crystals have been grown without a seed. The crystals show very low subgrain boundary structures with dislocation densities ranging from 5×10^4 cm^{-2} to 3×10^5 cm^{-2} as measured by the etch pit method. The electrical characteristics of smaller crystals (20 mm in diameter) grown by the traveling heater method have

DD FORM 1 JAN 73 1473 EDITION OF 1 NOV 65 IS OBSOLETE

UNCLASSIFIED

SECURITY CLASSIFICATION OF THIS PAGE (When Data Entered)

shown purification during growth. For n-type crystals with x = 0.24 to 0.25 carrier concentrations of $\sim 2 \times 10^{14}$ cm^{-3} and mobilities of 1.2×10^5 $cm^2/V \cdot second$ were measured at 77 K. Metal insulator semiconductor devices built on these crystals exhibit high-frequency C-V characteristics with dark currents within one order of magnitude of the Auger limit at 77 K.

Based on the metal insulator semiconductor device results and the electrical characteristics of oriented 20-mm-diameter crystals, the electrical characteristics of 40-mm-diameter crystals are expected to be equivalent, if not superior, because of reduced material handling.

TABLE OF CONTENTS

LIST OF ILLUSTRATIONS

SCIENTIFIC PERSONNEL SUPPORTED BY THIS PROJECT

L. Colombo	Program Manager and Principal Investigator
A.J. Syllaios	Investigator
R.W. Perlaky (1 November 1984—31 March 1985)	Investigator
M.M. Lopez (1 April 1984—1 February 1986)	Investigator

SECTION I

INTRODUCTION

This program is an extension of the 1982–1983 program, Contract Number MDA903–82C–0439, on the growth of 20-mm-diameter crystals by the incremental quenching technique. A synopsis of the accomplishments of the former program is given in Appendix A in the form of a paper published in the *Journal of Vacuum Science Technology*. Development of high quality, low cost (Hg,Cd)Te crystals for the next generation infrared (IR) detectors in the 8- to 12-μm spectral region depends on the availability of device quality and large area crystals. Bulk single-crystal growth is one way to achieve high purity and low point and extended defect density material.

The objective of this program was to establish the feasibility of large diameter (40 mm) growth of (Hg,Cd)Te single crystals. The technique that was investigated to accomplish this is the incremental rapid solidification of large volumes of (Hg,Cd)Te melts with subsequent crystal growth by the solid-state recrystallization technique. However, during the course of the program it became obvious that the traveling heater method (THM) would be a more controlled method of growing crystals using the incrementally quenched ingots. This method also allows purification during growth, as is clearly shown in Appendix B.

The incremental quenching technique is particularly suitable to solidify large volumes of material without large macroscopic segregation effects. The macroscopic compositional homogeneity makes this technique also useful for source material for growth of single crystals by both the traveling heater method and the solid-state recrystallization technique. Although microscopic segregation from supercooling the tellurium-rich melts are observed, the material is macroscopically uniform and can be easily used as a source material for growth by THM. This has several advantages, an important one being that the dissolving interface is macroscopically uniformly dissolved. This is not true if a composite material were used, as is the case with the technique used by Triboulet, et al.[5]

This report contains two basic sections, the quenching section and the growth of single crystals by the solid-state recrystallization technique and THM. There are also three appendixes discussing the growth of large diameter (20 mm) crystals by the incremental quenching method and the growth of 20-mm-diameter (Hg,Cd)Te, (Hg,Cd,Zn)Te and (Hg,Mn)Te by THM. The work in Appendixes B and C was done under IR&D funding and is meant to support the 40-mm-diameter development. That is, this work is a stepping stone to the development of high-quality 40-mm-diameter crystals.

SECTION II

PROGRAM SUMMARY

This section summarizes the most significant results of this research program and identifies problem areas that require further work.

A. INCREMENTAL QUENCHING PROCESS

Forty-mm-diameter polycrystalline ingots weighing up to 700 grams have been incrementally solidified in fused silica ampoules. This technique was used to provide source material for solid-state recrystallization experiments and growth of large diameter ingots by the THM.

The ingots were quenched in ampoules contained in a high pressure vessel at 650 to 700 psi and temperature up to 870°C. Two techniques were used to quench the ingots. One was to transfer the liquid into the transfer chamber at 650°C. The second was to transfer the liquid into the lower chamber while cooling the bottom of the ampoule with nitrogen gas flowing through a heat exchanger in intimate contact with a high conductivity graphite stem in contact with the ampoule. The lower chamber is used to both control the mercury vapor pressure over the melt and to provide a high temperature gradient through which the material can be quenched. These growth conditions were related to the thermal analysis and the boundary conditions to evaluate the thermal gradients within the ingot during quenching and the cooldown phase after complete material transfer.

Solid ingots with a bimodal microstructure were quenched. The unidirectional heat extraction under the prevailing growth conditions and furnace mass did not cause any microstructural homogeneity improvement. Also when high flow rates were used, the ingot was very weak and crumbled very easily. Ingots quenched without intentional heat extraction produced whole ingots without any cracks.

The ingots were typically quenched under the following conditions:

Liquid temperature	T_l = 835°C
Transfer chamber	T_s = 650°C
Orifice diameter	2a = 1.5 mm
Excess mercury	0.02 gm/cc (free sodium)

The material was characterized by standard metallurgical techniques to evaluate the microstructure and the thermal gradients within the ingot during the quenching process.

B. RECRYSTALLIZATION

Recrystallization of these large ingots has been extremely difficult because of high mercury vapor pressure and the expected anomalous behavior of the grain growth process. Grains as large as 25 mm were grown after 1 month at 660°C under two zone conditions with a mercury vapor pressure of 20 atmospheres. However, the crystal contained a large number of voids up to about 1 mm. Experiments to establish exact grain growth conditions have been very difficult to complete because of frequent explosions of the ampoules in the high-pressure vessel during recrystallization.

C. GROWTH BY THE TRAVELING HEATER METHOD

THM has been used as a low-temperature growth technique to grow 40-mm-diameter ingots. Two three-zone furnaces were built with temperature control of ±0.5°C and temperature gradients of 50° to 120°C cm. Ingots were grown with varying temperature gradients and ampoule tip shape. For ampoules with pointed tips, it was found that the initial interface was highly concave giving rise to ingots with small

crystallites whereas crystals grown with a flat bottom gave rise to larger crystals. The concavity of the interface was found to be affected by both radiation cooling in a nonaxial direction as well as the high liquid to solid thermal conductivity. The microstructure within the grains for ingots grown in ampoules with a flat bottom showed a low dislocation density and a low subgrain boundary density. The interface shape was related to the microstructure of the growing ingot. At high radii of curvature (e.g., at the ampoule wall/solid interface) the subgrain boundary density is higher than at the center of the crystal.

The melt/solid interface is an extremely important factor in the growth of high quality (Hg,Cd)Te crystals by any melt growth technique. Because of the clear microstructural difference of the growing ingot and the solvent (i.e., the tellurium rich solution), the interface is clearly marked by the eutectic/single-phase microstructure. This has made crystal growth evaluation and microstructure evolution much easier.

Seeding of the (Hg,Cd)Te provides an easy way to select growth direction. In nonseeded growth runs with a flat-bottomed ampoule, there was no clear grain selection, although the majority of the grains were equiaxed as determined from dislocation etch pit shape. During this investigation, several seeding techniques were investigated. However, initial temperature control difficulties at the seed made partial seed dissolution difficult. Experiments are currently under way to address the difficulties experienced in controlled seed dissolution. Reproducible growth of oriented 20-mm-diameter crystals indicate that this should not be a problem.

D. ELECTRICAL AND DEVICE PROPERTIES

Forty-millimeter-diameter crystals grown so far has not yet been characterized by Hall-effect measurements nor have any devices been built on the wafers. However, as shown in Appendixes B and C, 20-mm-diameter (Hg,Cd)Te, (Hg,Cd,Zn)Te, and (Hg,Mn)Te crystals have been characterized by both the Hall-effect and MIS device performance. The Hall-effect measurements, together with the device performance and electrical data of crystals grown by the solid-state recrystallization technique using the same starting materials, indicate that purification is taking place during growth. Carrier concentrations of 2×10^{14} cm^{-3} are obtained with mobilities of 1.2×10^5 cm^2/V·second at 77 K for $x = 0.24$ with the transport properties showing a classical behavior as a function of temperature. MIS devices built on these crystals were evaluated at 77 K. High frequency C-V characteristics were observed uniformly across the ingot with dark currents ranging from 1 to 10 μA/cm^2 for $\lambda_{co} = 8.3$ μm at 77 K. The carrier concentration calculated from C-V curves was 3 to 4 $\times 10^{14}$ cm^{-3} at 77 K.

SECTION III

CRYSTAL GROWTH

The crystal growth process for 40-mm-diameter crystals is divided into two phases. The first phase consists of a polycrystalline ingot growth by the incremental quenching technique where a large melt is sequentially solidified into a fused silica chamber. The second phase of the growth process consists of a recrystallization phase and growth THM. In this section, the quenching process is described and a thermal analysis is presented to clarify the thermal losses and profile of the growing ingot during quenching. Then the recrystallization and the growth by THM are described.

A. INCREMENTAL QUENCHING

1. Ingot Growth

To solidify large melts of (Hg,Cd)Te, the liquid material is slowly transferred in small amounts from a hot chamber at a temperature above the liquidus to a chamber at a temperature below the solidus through a small orifice. Figure 1 schematically shows the incremental quenching process. Because of the high mercury vapor pressure typically above 45 atm for x = 0.22, over the (Hg,Cd)Te melt, the fused silica ampoule is contained in high pressure vessel to prevent explosions. Figure 2 shows the high pressure vessel used to incrementally quench the 40-mm-diameter ingots.

Quenching of large melts also requires an appropriate melt chamber design to contain large quantities of the starting material while minimizing the overall ampoule volume to reduce fused silica cost and to fit the furnace profile. Figure 3 shows a macrograph of the incremental quench ampoule containing the appropriate amounts of Hg, Cd, and Te. The current ampoule design and loading process allows over 700 grams of $Hg_{0.78}Cd_{0.22}Te$ to be loaded. This yields an ingot that is approximately 3 inches long.

A flowchart of the incremental quench process is shown in Figure 4. The most critical phase of the quenching process is the liquid transfer stage. The temperature of the ingot cannot exceed the solidus temperature. This is controlled by the transfer rate and the transfer chamber temperature. The orifice temperature during the quenching is also carefully kept between 825° and 830°C to allow the liquid to transfer. Any large compositional inhomogeneities in the melt are automatically screened out by the orifice. If the temperature within the melt is such that the composition is more than 0.24, the material will not transfer through the orifice. The temperature of the solidification chamber and the melt temperature during the transfer are extremely critical. When the temperature of the bottom chamber is higher than 665°C, large voids are observed in the ingot. Too low a transfer chamber temperature yields ingots with large voids, principally at the center of the ingot indicating coring as a result of high radial heat transfer rates. Another important parameter is the excess mercury content. Under the same thermal profile, a high excess mercury content gives rise to intergranular mercury, which causes the ingot to crumble and, as shown in the case of the smaller ingots (20-mm-diameter), low-grain growth rates are usually observed under these conditions.

The solidification conditions for the large diameter ingots were found to be very close to those determined for the 20-mm-diameter ingots reported in a previous program under Contract No. MDA903-82-C-0439 (Appendix A). However, because of the large mass of material solidified, the temperature of the solidification chamber was held between 640° and 650°C rather than 665°C used for the 20-mm-diameter ingots. In addition, the revised reaction chamber design allowed the orifice diameter to be controlled with greater precision than in the growth of 20-mm-diameter ingots. As a result, the microstructure uniformity from ingot to ingot was greatly improved, the ampoules could be more easily cleaned, and the reaction chamber could be reused. The following thermophysical conditions have yielded reproducible void-free ingots that are 40 mm in diameter and 75 mm long:

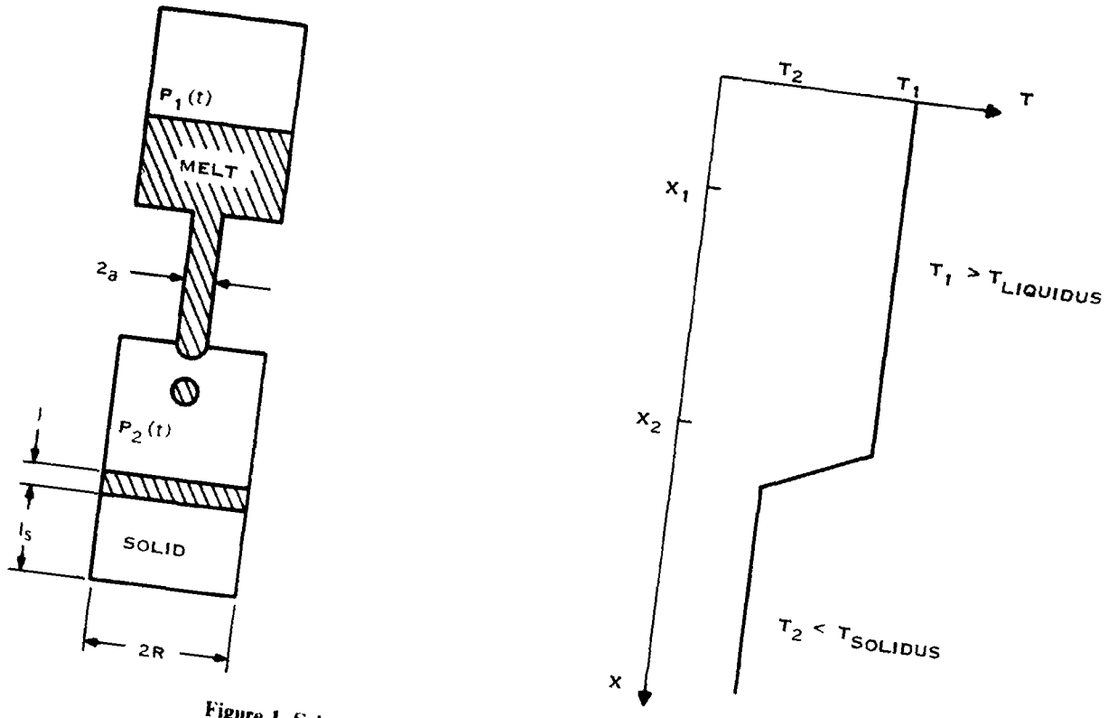

Figure 1. Schematic Diagram of the Incremental Quench Process

295118

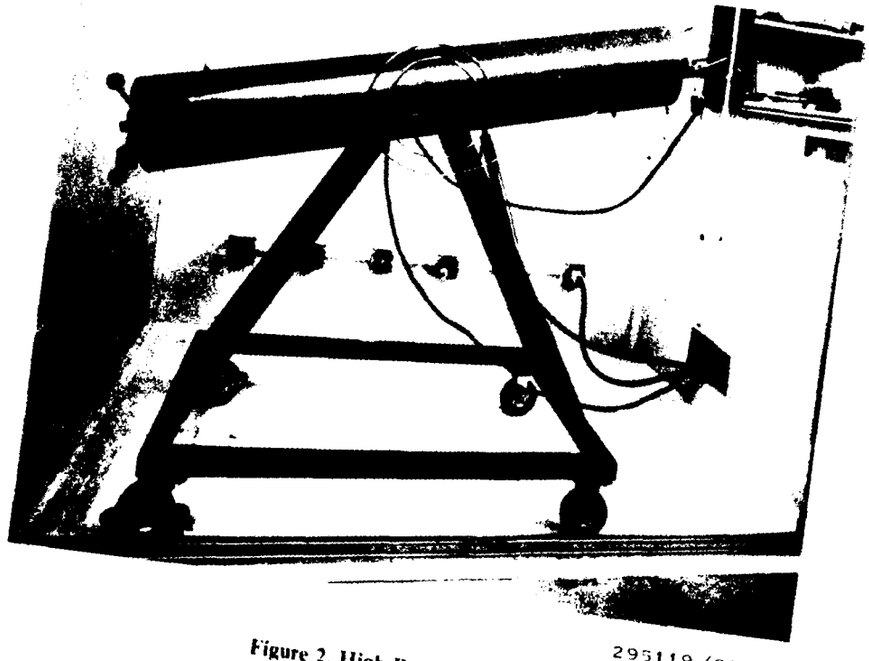

Figure 2. High-Pressure Vessel

295119 (88-62)

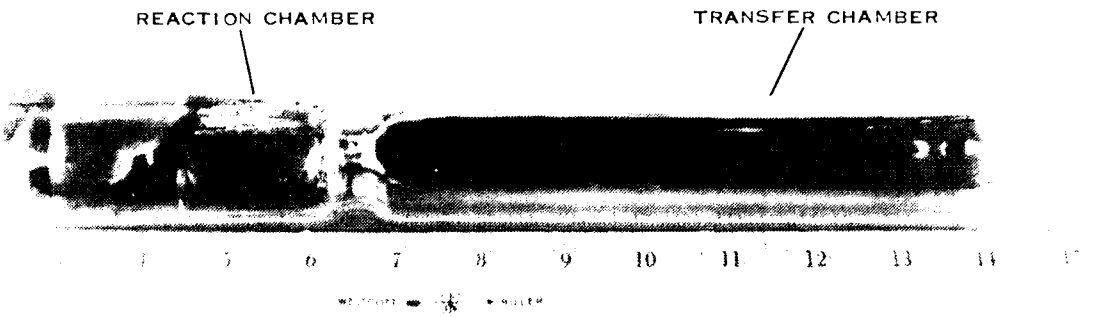

295120

Figure 3. Loaded Incremental Quench Ampoule

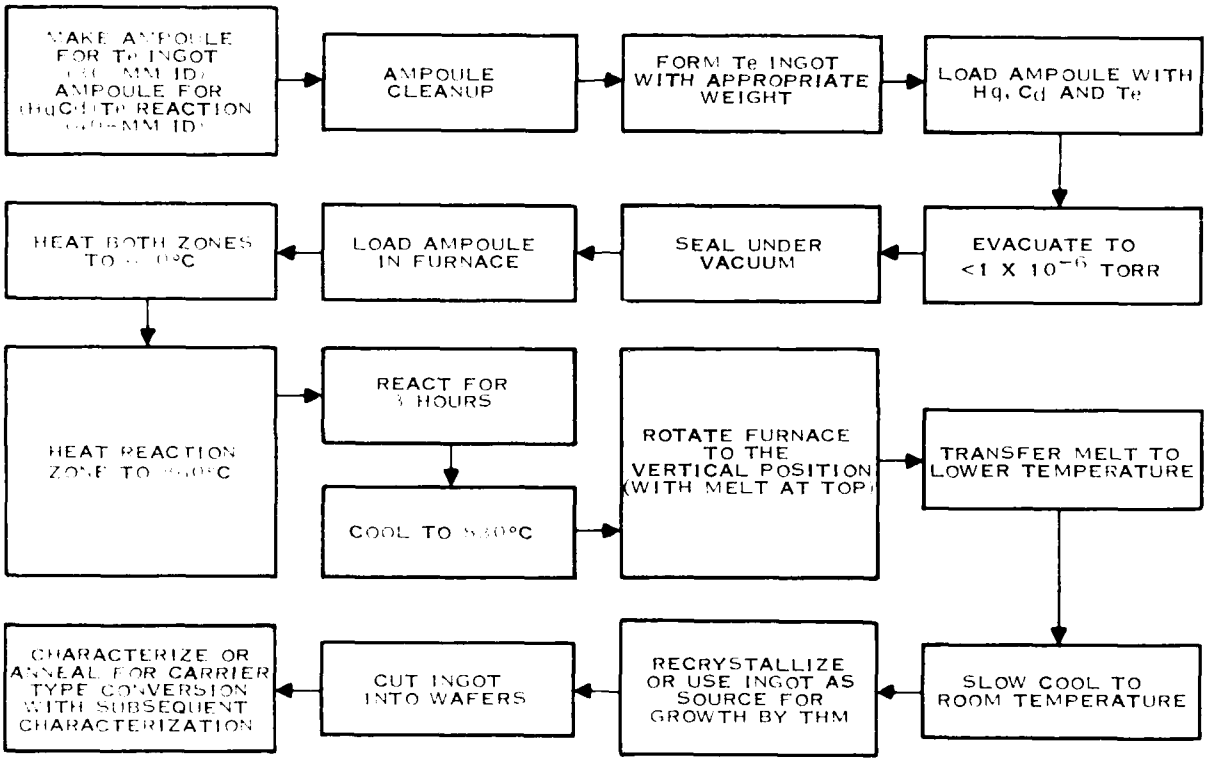

29 4121

Figure 4. Flowchart of the Incremental Quench Process

T(liquid)	825 to 830 C
T(solidification chamber)	640 to 650 C
Orifice diameter (2a)	1.5 mm
Excess mercury	0.02 gm cc

2. Microstructure and Temperature Distribution

The microstructure of the solidified ingot was studied by chemical etching techniques. This analysis provides information not only on the microstructural homogeneity but also provides qualitative information on the temperature distribution within the ingot during the solidification stage. This, together with the two-dimensional thermal analysis, provides information on the cooling mechanism of the solidified ingot and direction on how to optimize thermal management during solidification.

Figure 5 shows the microstructure of the incrementally quenched ingot as a function of distance away from the ampoule surface. The grain size near the surface is very small and it slowly increases toward the center of the ingot. Dendrites are also observed at the center of the ingot. This can be explained by the existence of a temperature gradient within the solidifying material (i.e., as the material is transferred, the thermal losses occur both radially and axially). The microstructure of the ingot is dominated by radial rather than axial heat transfer because of the low thermal conductivity of the solidifying (Hg,Cd)Te ingot. The thermal losses in the radial direction occur by both radiation loss and by convection through the high pressure helium gas surrounding the ampoule. This can be more clearly seen in the temperature profile calculated by the two-dimensional thermal analysis shown in the following subsection. Only when axial heat transfer is maximized, the ingot shows low temperature gradients across the diameter of the ingot. A cellular structure is always uniformly observed at the top and bottom of the ingot. Increased heat transfer rates at the surface improves the microstructural uniformity in these areas. At the top of the ingot, radiation cooling dominates; conduction through the fused silica and through the graphite stem in contact with the furnace end at the bottom of the ingot.

3. Thermal Analysis

As discussed in the previous subsection, the microstructure of the incrementally quenched (Hg,Cd)Te ingot is influenced by the temperature gradients that exist at the solid-liquid interface. The temperature gradients and temperature profiles in the ingot are calculated for the simplified cases of steady-state heat flow regimes for one- and two-dimensional cases. It is assumed that the thermal conductivities of the melt and solid (Hg,Cd)Te are equal and temperature independent. Convection heat transfer in the melt is neglected.

a. One-Dimensional Thermal Analysis

The steady-state heat transfer equation in one dimension may be written as

$$\frac{d^2 T(z)}{dz^2} + q'''/k = 0 \tag{1}$$

where $T(z)$ is the temperature in the ingot and k is the thermal conductivity. The heat dissipated per unit area as depicted in Figure 6 is equal to

$$q''' = \frac{2 h \pi R(T - T_0)dz}{\pi R^2 dz} \tag{2}$$

Here, h is the convection heat-transfer coefficient to the environment temperature T_0, and R is the radius of the of the ingot.

The heat dissipated at the base of the ingot ($z = L$) assuming convection heat transfer is given by:

$$q_b = -k(dT/dz)_{z=L} = h(T - T_0) \tag{3}$$

The heat flow Equation (1) is subject to the boundary condition

$$T = T_1 \text{ at } z = 0 \tag{4}$$

i.e., the temperature at the top of the ingot is held constant and equal to the melt temperature T_1.

From the theory of fins [Equation (1)], the solution of the differential Equation (1) is

$$T = T_0 + (T_e - T_0)\left[\frac{\cosh [m(L - z)] + n \sinh [m(L - z)]}{\cosh (mL) + n \sinh (mL)}\right] \tag{5}$$

with $m^2 = h/kR$; $n = h/mk$.

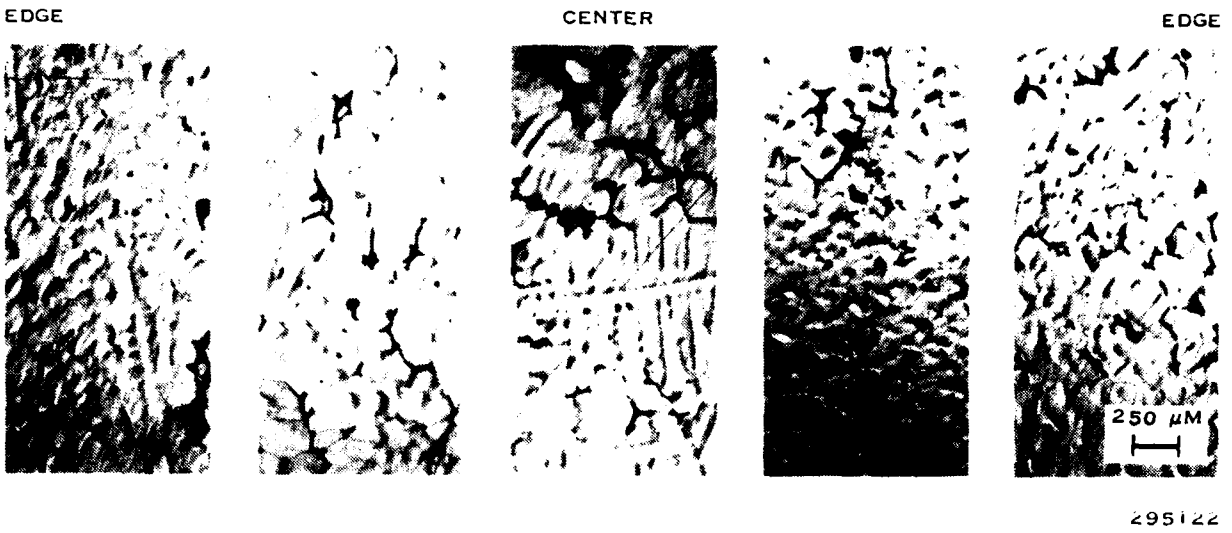

Figure 5. Microstructure of an Incrementally Quenched Ingot as a Function of Distance Across the Ingot One-Dimensional Heat Flow Geometry

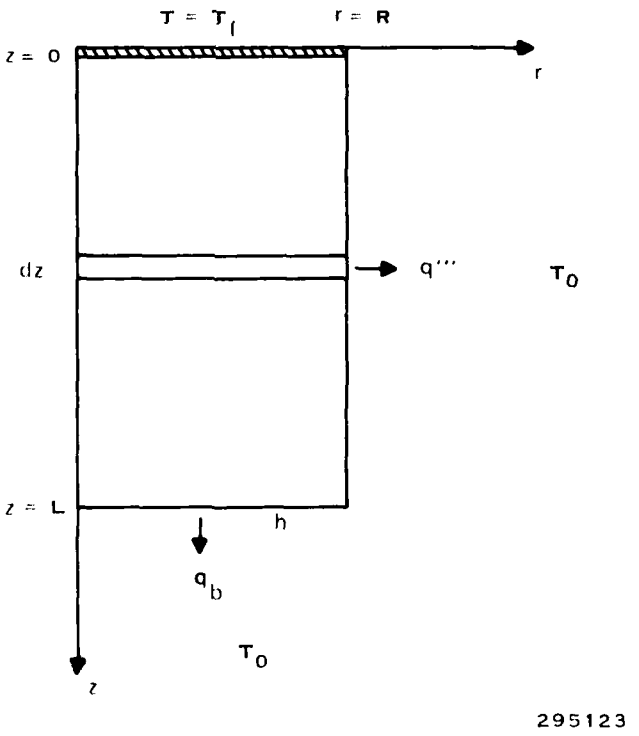

Figure 6. One-Dimensional Heat Flow Geometry

The temperature distribution from Equation (5) is plotted in Figure 7(A) with the heat-transfer coefficient, h, as a parameter and Figure 7(B) with the ingot length L as a parameter. It is seen that the (axial) temperature gradient at the interface (denoted by the solid temperature) decreases with decreasing heat-transfer coefficient; i.e., by approaching adiabatic conditions. The gradient is also decreasing with increasing ingot length and the axial component of the heat flow becomes larger.

b. Two-Dimensional Analysis

The steady-state heat-transfer equation in cylindrical coordinates with rotational symmetry given by

$$\frac{\partial^2 T}{\partial r^2} + \frac{1}{r}\frac{\partial T}{\partial r} + \frac{\partial^2 T}{\partial z^2} = 0 \qquad (6)$$

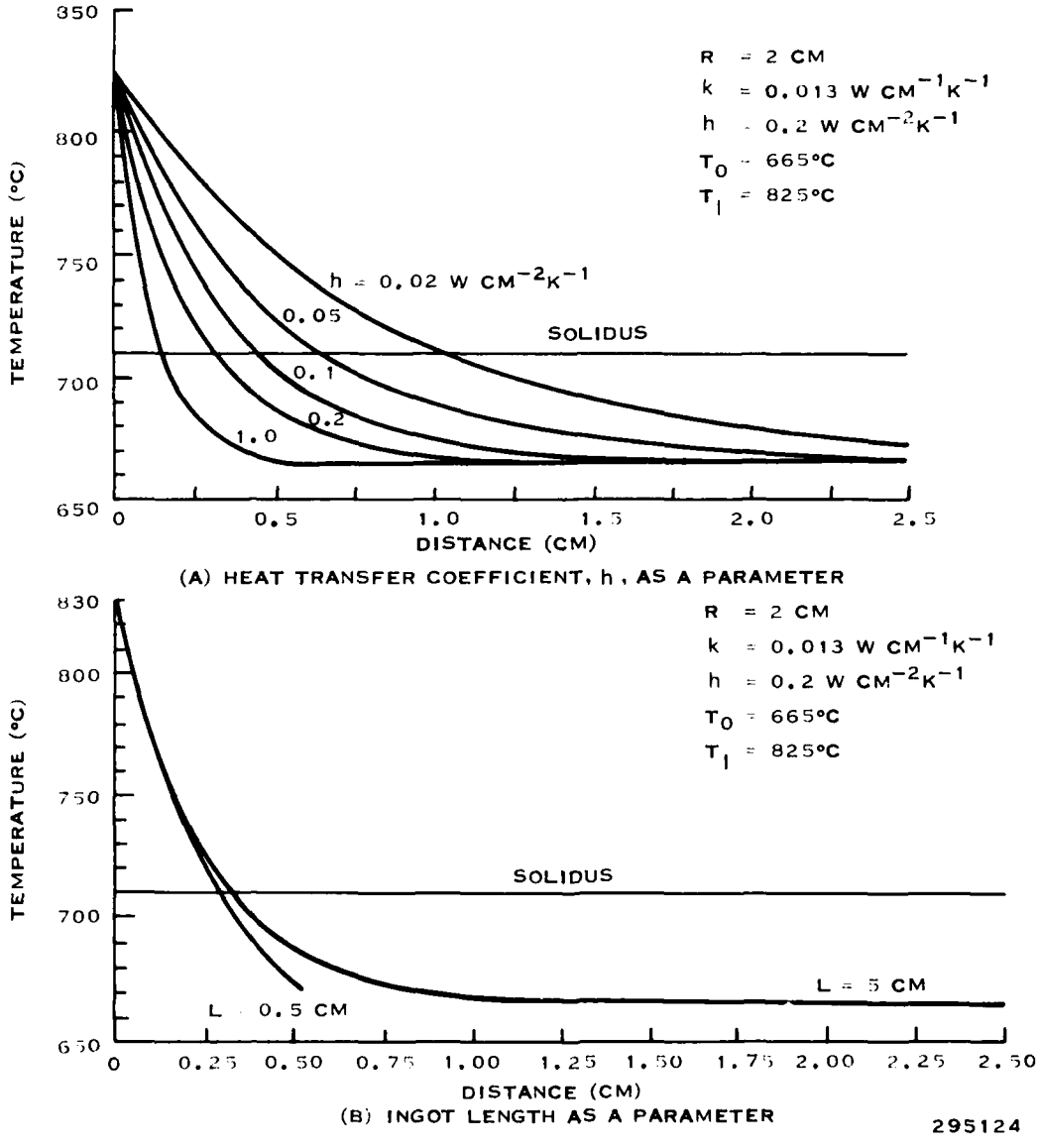

Figure 7. Temperature Profile of (Hg,Cd)Te Ingot From One-Dimensional Thermal Analysis

The boundary conditions as shown in Figure 8 are:

Top surface: $z = 0$; prescribed temperature: $T = T_l$ (liquid)

Bottom surface: $z = L$; prescribed temperature: $T = T_b$

Axial line: $r = 0, 0 \leq z \leq L$; $\partial T/\partial r = 0$

Side surface: $r = R$; $0 \leq z \leq L$; $Q_{out} = -K_s\, \partial T/\partial r = \sigma\epsilon_B(T^4 - T_0^4) + h(T - T_0)$

Flux condition at liquid-solid interface:

$$k\, \partial T/\partial n = k_s\, \partial T_s/\partial n$$

As for the one-dimensional case again the melt and solid thermal conductivities were assumed to be the same. This is convenient for the numerical computation because in that case the temperature behaves as if no interface were present.

Equation (6), the Laplace equation, was solved by the finite difference method using forward differences and the Gauss Seidel/successive overelaxation iteration technique. The results are shown in Figure 9 where the isotherms are plotted for two values of the heat-transfer coefficient, h, and two values of the bottom temperature, T_{bottom}. The radial dependence of the isotherms is minimized when the radial heat transfer is minimized (small heat-transfer coefficient) and the axial heat flow is maximized (low bottom temperature).

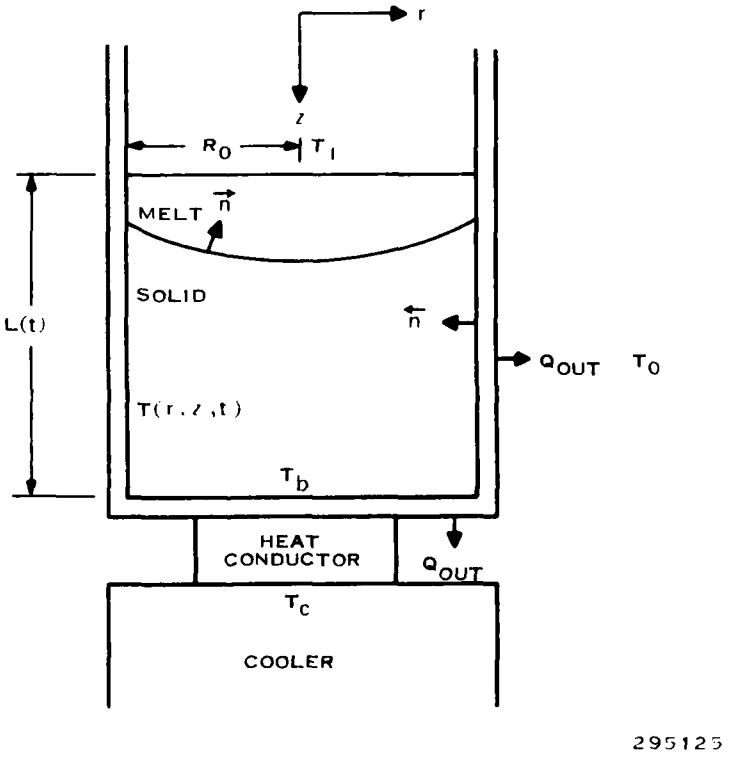

Figure 8. Two-Dimensional Heat Flow Geometry

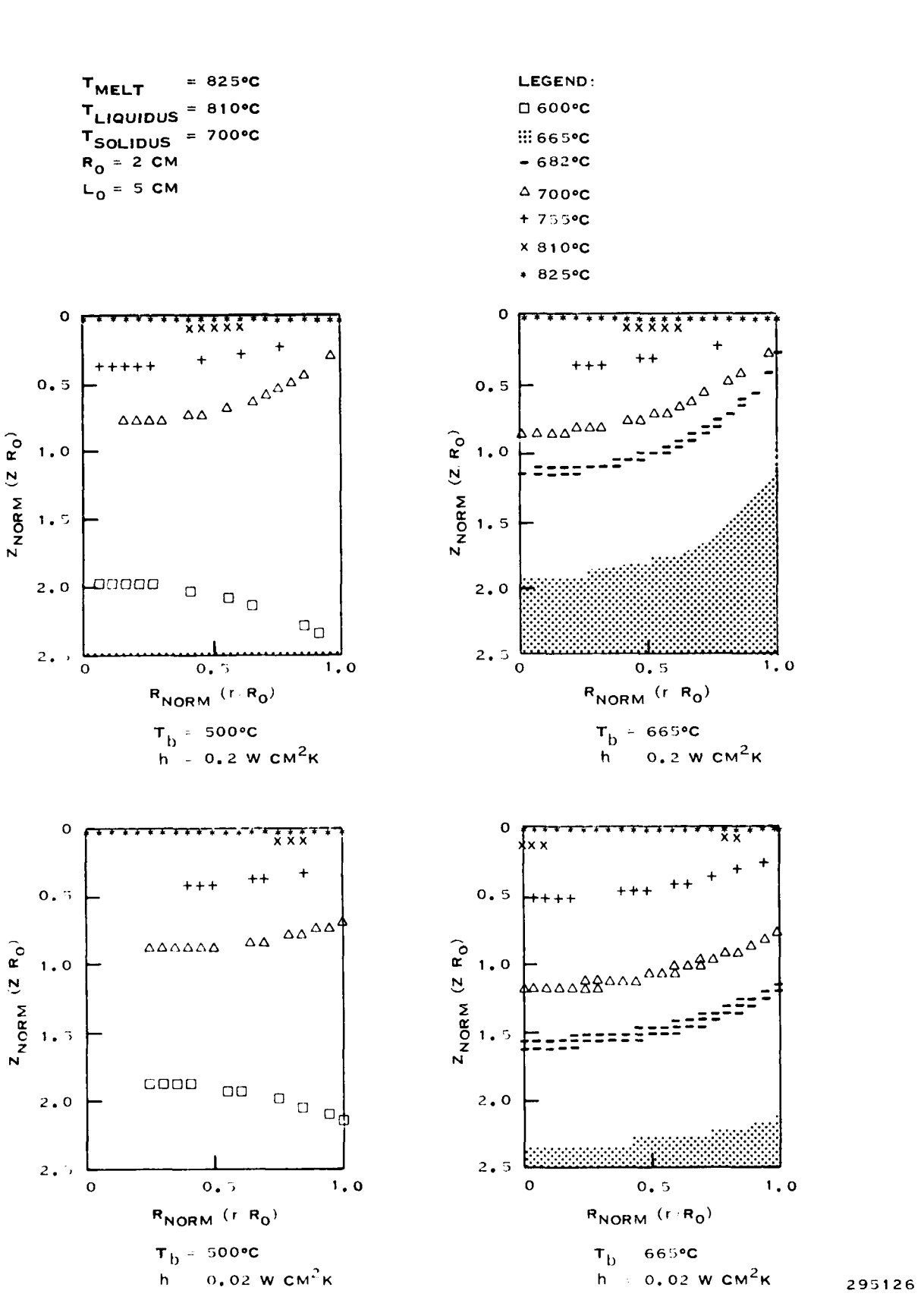

Figure 9. Calculated Isotherms in (Hg,Cd)Te Ingots

B. RECRYSTALLIZATION

Grain growth of the large diameter ingots has been very difficult for several reasons. The large volume and large diameter require that the ingots be contained in a high-pressure vessel. The high-pressure vessels used were externally heated and could be pressurized up to 500 psi at the operating temperature, 665°C. Under these conditions, the fused silica ampoule is highly stressed and after a few weeks it explodes. Many ingots have been lost because of explosions. When recrystallization for 28 days is accomplished without explosions, the fused silica ampoules have always imploded upon sawing to remove the ingot. Because the implosions were not expected, they posed a danger for the first few ingots grown.

Growth of the smaller diameter ingots (20 mm) showed a time dependence with an exponent larger than the theoretical 0.5. This was attributed to an anomalous grain growth occurring in the presence of an optimum amount of liquid phase. In the case of the 40-mm-diameter crystal, anomalous grain growth is also observed; however, the presence of an excessive amount of second phase and voids has caused the ingots to have only partially exhibited anomalous grain growth. The part of the ingot having smaller grain invariably contained an intergranular second phase and voids. This weakened the ingots to the point that the polycrystalline part crumbled. Figure 10 shows the grain diameter as a function of recrystallization time at 665°C for both the 20-mm-diameter ingots grown during the previous DARPA program and the 40-mm-diameter ingot. The 20-mm-diameter ingots statistically contained few holes and had large grains. A critical amount of second-phase, tellurium-rich liquid is observed and is believed to be responsible for the anomalous grain growth. Explosions have made overall grain growth in the large diameter crystals difficult to optimize.

The microstructure of the recrystallized ingots showed a low subgrain boundary structure and a dislocation density in the range of about 3×10^5 cm^{-2}. Unlike CdTe, no twins have been observed, although twins have been observed occasionally in the 20-mm-diameter crystals. Figure 11 shows the macrostructure and the microstructure of an ingot annealed for 28 days under two zone conditions, with the ingot held at 660°C and the mercury reservoir at 600°C. The microstructure analysis shows a higher dislocation and subgrain boundary density than material grown by THM. Dislocation nesting is observed in areas where there is a high subgrain boundary density. The basic difference between SSR and THM grown material is that, in the case of THM, the microstructure can more easily be related to prevailing growth conditions. In material grown by the SSR process, growth kinetics and microstructure evolution are controlled by both the stoichiometry during recrystallization and reaction and the as-quenched microstructure. This makes control much more difficult.

C. GROWTH BY THE TRAVELING HEATER METHOD

The THM has been used to grow large diameter ingots at low temperatures. For a review of the principles of THM, see Reference 1. The following list contains the principal incentives for using this technique to grow the crystals:

- Low temperature growth
- Low mercury vapor pressure
- Seeded growth
- Purification during growth
- Near equilibrium growth
- Growth kinetics control
- Use of known tellurium-rich corner of the phase diagram.

A furnace whose schematic diagram is shown in Figure 12 was used to grow the large diameter crystal. The furnace consists of a central heater water cooled on both sides with heaters on each side to control the temperature gradient at the growing and dissolving interfaces. The growth of large diameter uniform

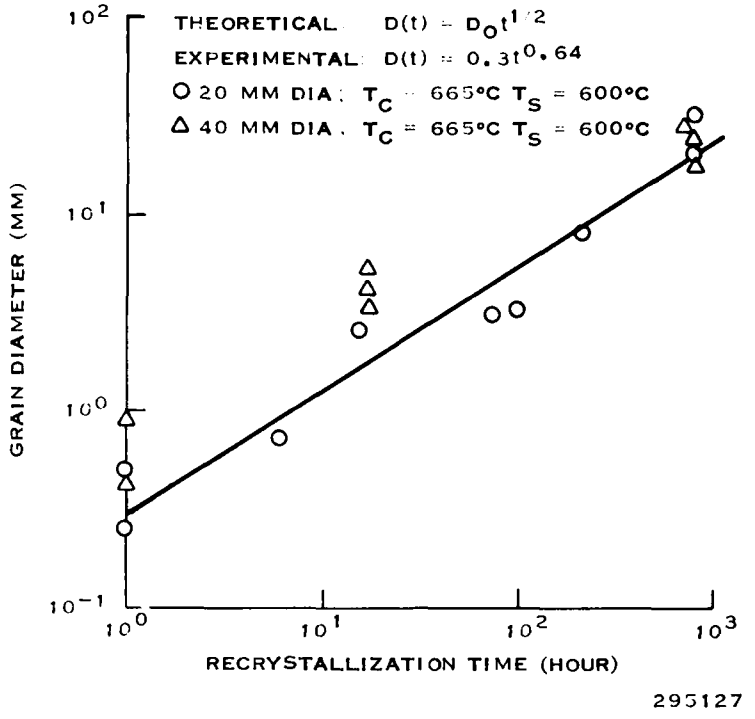

Figure 10. Grain Size of Recrystallized Ingots as a Function of Time

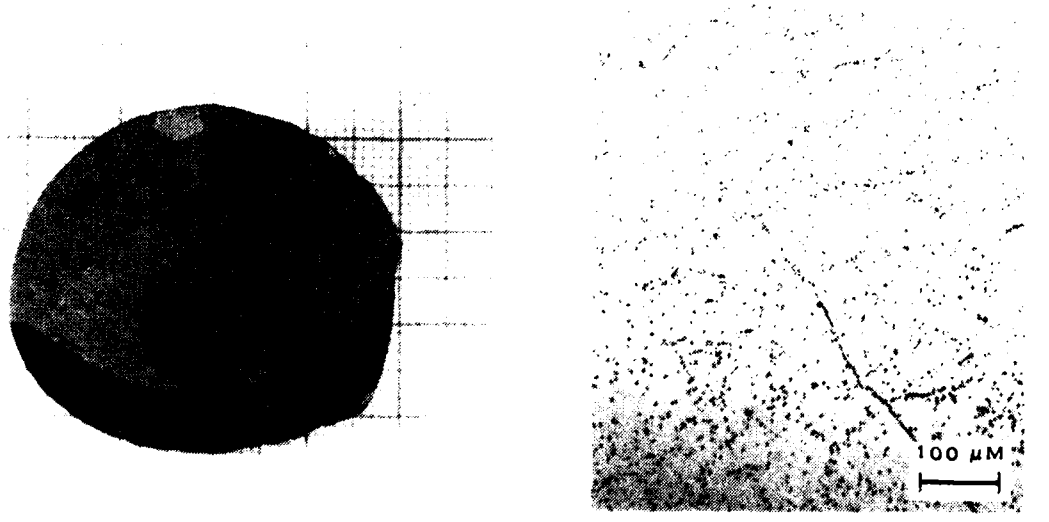

Figure 11. Microstructure and Macrostructure of Recrystallized (Hg,Cd)Te Ingot

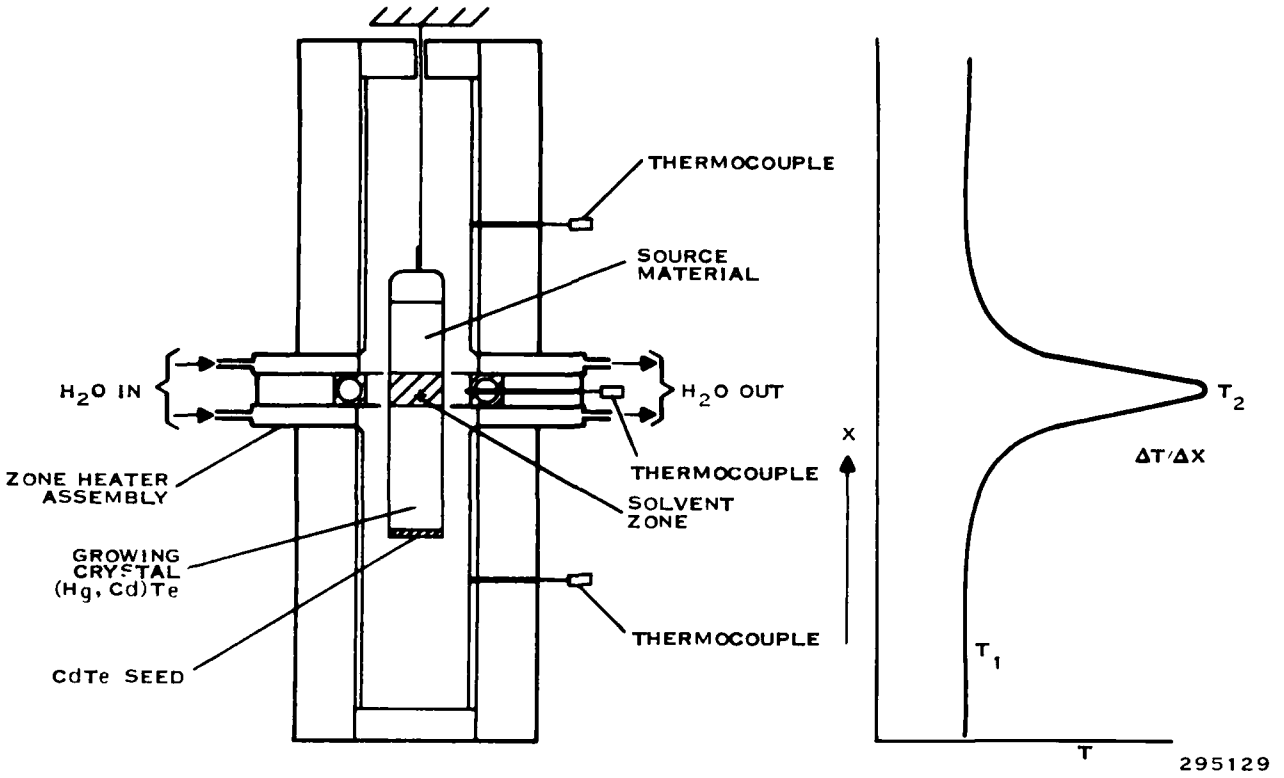

Figure 12. Three-Zone Furnace Used To Grow (Hg,Cd)Te Crystals by THM

single crystals of (Hg,Cd)Te requires development of efficient thermal control and an understanding of the basic thermal processes during growth. Furnace design, fabrication, and temperature control are crucial to successful growth by THM.

The as-quenched (Hg,Cd)Te polycrystalline ingots are used as the source material once the ingot has been lapped and cleaned on one side to ensure a flat surface. The solvent is reacted separately to an appropriate size to match the furnace profile. The solvent composition was determined from the liquidus isotherms and isoconcentration lines shown in Figure 13. The solvent and the source are then loaded into an ampoule as shown in Figure 14, evacuated, and sealed. The initial experiments were done using ampoules with a pointed tip to attempt self seeding, but as it will be shown self seeding is not an appropriate way to grow single crystal (Hg,Cd)Te (Appendix C).

Efficient and controlled axial heat transfer at the liquid-solid interface requires an optimum furnace design and a knowledge of the solvent and growing solid thermal properties together with the ampoule. Figure 15 shows schematically how some basic ideas were used to design the multizone furnace. The temperature gradient can be varied by varying the chilled water flow rate and the side heater temperature. In addition to the furnace design, ampoule design was found to be extremely important for single-crystal growth especially at the beginning of the growth. Ampoule end effects were found to be the determining factor in whether or not a flat interface was achieved. (Also see Appendix C for the effect of ampoule end shape on the interface shape.)

The following factors were found to greatly affect the liquid-solid interface:

Ampoule end shape
Growth rate
Gradient at growing interface
ΔT between the cold and hot zone

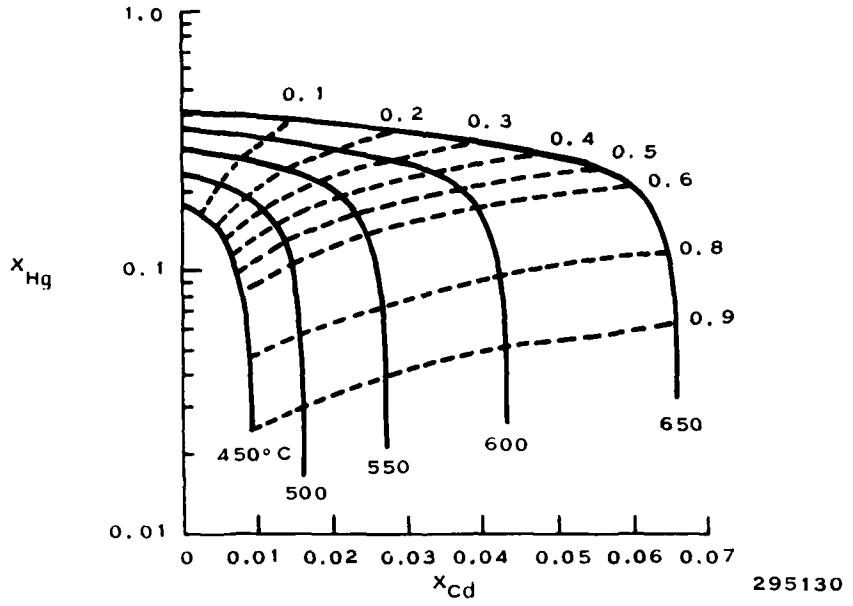

Figure 13. Liquidus and Isoconcentration Lines of the Te-Rich Side of the Ternary Hg-Cd-Te Phase Diagram

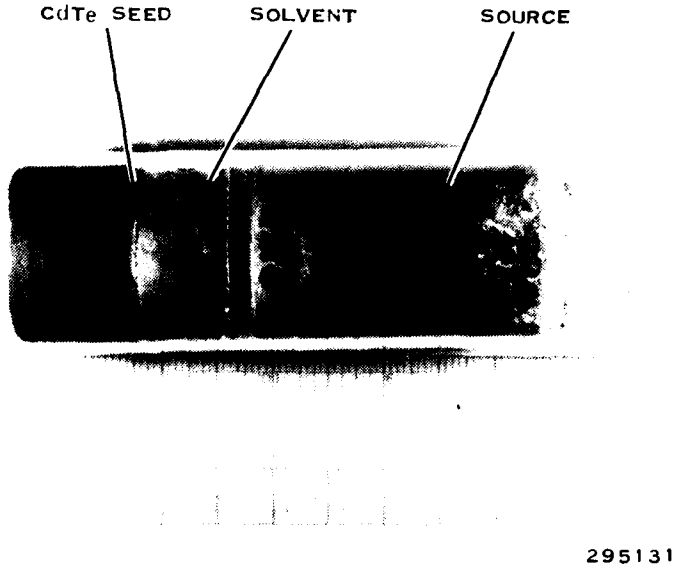

Figure 14. Loaded THM Ampoule Showing the CdTe Seed, the Solvent, and the Incrementally Quenched Source Material (Scale in Inches)

Thermal and optical properties of the ampoule
Communication between the central zone and the side heaters.

These are engineering problems that once clearly identified, should in principle be solved. However, one important parameter, thermal conductivity, plays a very important role in the interface shape. The thermal conductivity of the material, both the solvent and the solid, has the dominant effect and, since it is a physical property of the material, it cannot be changed. In this program, a tellurium-rich solution with mercury and cadmium was chosen as the solvent because of the availability of the thermodynamic data. An alternative approach would be the use of different solvents to match the thermal conductivity to that of the growing crystal. This would reduce the interface effect also observed in (Hg,Cd)Te grown by the Bridgman technique by Lehoczky and Szofran (Reference 2). Use of alternate solvents, however, requires a redetermination of the phase diagram for each solvent. A second parameter that has not been

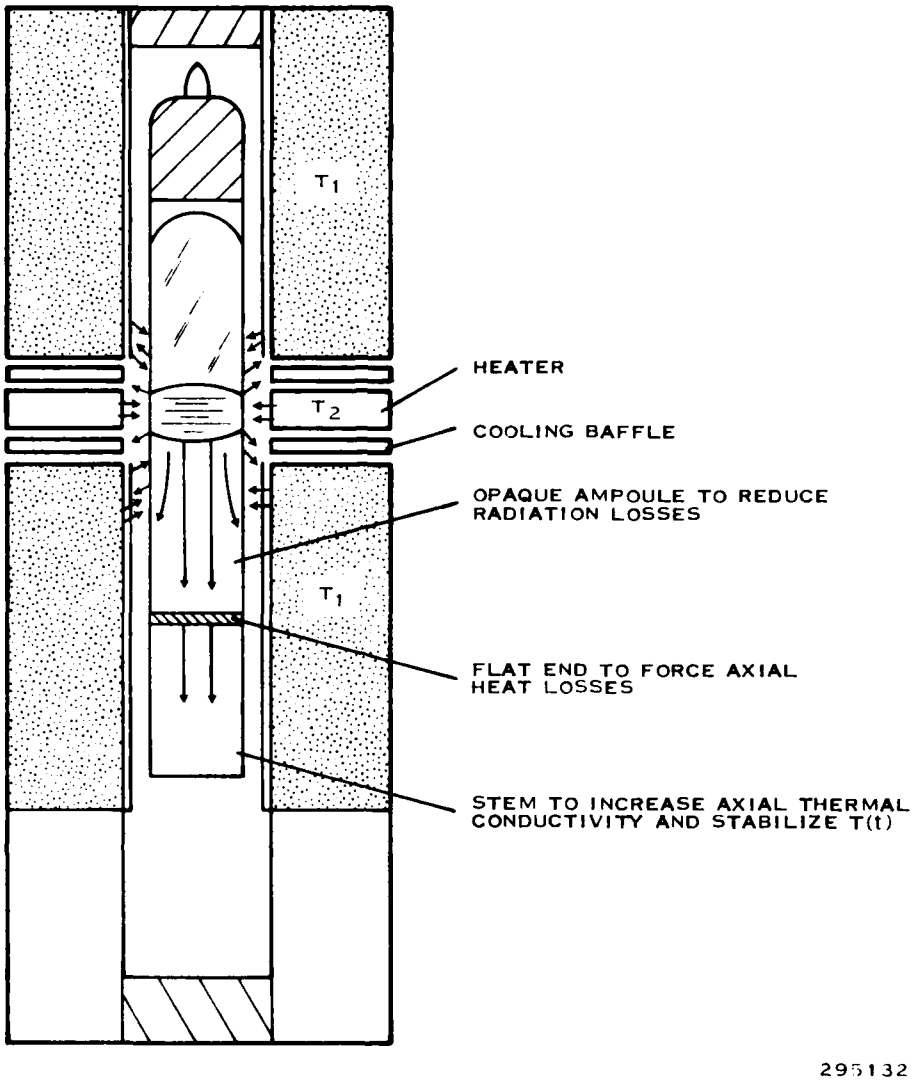

Figure 15. Thermal Flow Patterns in (Hg,Cd)Te/Te-Rich Solvent During Growth in a Three-Zone Furnace

investigated and needs consideration is the heat source. In our case, resistive heating was used. A combination of r–f and resistive or radiant heating may be the optimum way to create appropriate thermal profiles to control the liquid-solid interface and line and point defect densities.

The initial liquid/solid interface has been influenced by placing a graphite stem so as to promote high axial heat transfer. Furnace profile and temperature control becomes extremely critical since the temperature gradient under these conditions may vary with time. But as in the case of the 20-mm-diameter crystals, a planar initial interface is generated at the growth temperature of 500°C. Most of our growth rates have ranged from 2 to 3 mm/day at 500°C. In the case of 2 mm/day, the interface shape even at long distances (4.5 cm from the ampoule end; i.e., the starting point) maintains an interface close to planar except at the ampoule wall/crystal interface. Growth rates much higher than 3 mm/day tend to create larger interface concavity and melt retention is observed especially at the center of the ingot.

As in the case of the 20-mm-diameter growth, self-seeding geometries for growth of these systems, where the thermal conductivity of the melt is higher than that of the solid, give rise to highly concave interfaces. This is excentuated by nonaxial thermal losses by radiation through the ampoule wall. This is clearly shown in Figure 16(A), where the macrostructure of two ingots grown in a pointed and flat bottom ampoule are compared.

The solvent zone width in all the growth experiments has been about 1.5 to 2 cm. Under these conditions, the growth rate is controlled by thermal convection currents and diffusion because of the transport of mercury and cadmium from the dissolving to the growing interface. Although a narrow solvent zone is preferable for high growth rates, there are some physical limitations with the current furnace design. In the case of wide solvent zone widths, purification can be more easily achieved because the solvent does not become saturated with impurities. With a 15- to 20-mm solvent zone width, the dissolving interface is nearly flat and the growing interface away from the bottom of the ampoule is concave under the current growth conditions far away from the starting point. Microstructural analysis of the solid solvent after growth indicates that axial heat transfer is occurring away from the ampoule walls. This is exhibited by the dendritic alignment parallel to the growth axis.

The temperature during growth is controlled to better than 0.5°C. The gradient on both the dissolving interface and the growing interface has been controlled by chilled water and can be varied up to 120°C/cm. The microstructure, as expected, has been highly influenced by the temperature gradient. In the case where the temperature gradient is lower than 50°C/cm, a two-phase material consisting of (Hg,Cd)Te and (Hg,Cd)Te-Te eutectic structure is observed (Figure 17). This occurs as a result of constitutional supercooling. Under these conditions, impurities can also be trapped and may be located within the ingot in a periodic fashion according to the growth rate as a function of time. In (Hg,Mn)Te where the material is not as pure as (Hg,Cd)Te, there are microstructural indications that this might be occurring even in cases where solvent inclusions are not observed. Refer to Appendix C. When the gradient is increased to over 70°C/cm in air, a single-phase material is grown. Under these conditions, the dislocation density is found to be in the range of 5×10^4 to 2×10^5 cm^{-2}. A histogram of the dislocation density in the radial direction is shown in Figure 18. Although the ingot is not single crystal since it was not seeded, the microstructure shows very few subgrain boundaries as shown in Figure 19. This has been observed in many ingots, both 20- and 40-mm diameter. A higher density of subgrain boundaries is observed near the ampoule surface. This is associated with the higher concavity of the interface near the ampoule wall (i.e., a higher nucleation site density).

An initial goal of the revised program was to grow oriented single crystals by THM. Self-seeding geometries as already mentioned are not amenable to single-crystal growth. Two seeding techniques have been investigated. First, a 20-μm-thick CdTe film on sapphire grown by MOCVD was used. Here the idea was to accomplish one of two objectives. Either use the CdTe film as the seed or, if the film were to dissolve, use the sapphire to seed the (Hg,Cd)Te. The CdTe film dissolved but (Hg,Cd)Te did not grow epitaxially as hoped. A second technique to seed the crystal was to use a CdTe seed oriented in the (111) direction. The seed thicknesses were approximately 2-mm and 40-mm diameter. The initial experiments to seed into the CdTe have not been successful because of complete seed dissolution in one case and no dissolution in the other. Figure 16(B) shows a macrograph of an ingot grown under the preceding conditions. The grains are about 20 mm in diameter and as long as 40 mm. In addition, the microstructure shows a low dislocation density with large areas of substructure-free material. Other geometries and improved temperature control at the seed surface are currently under development.

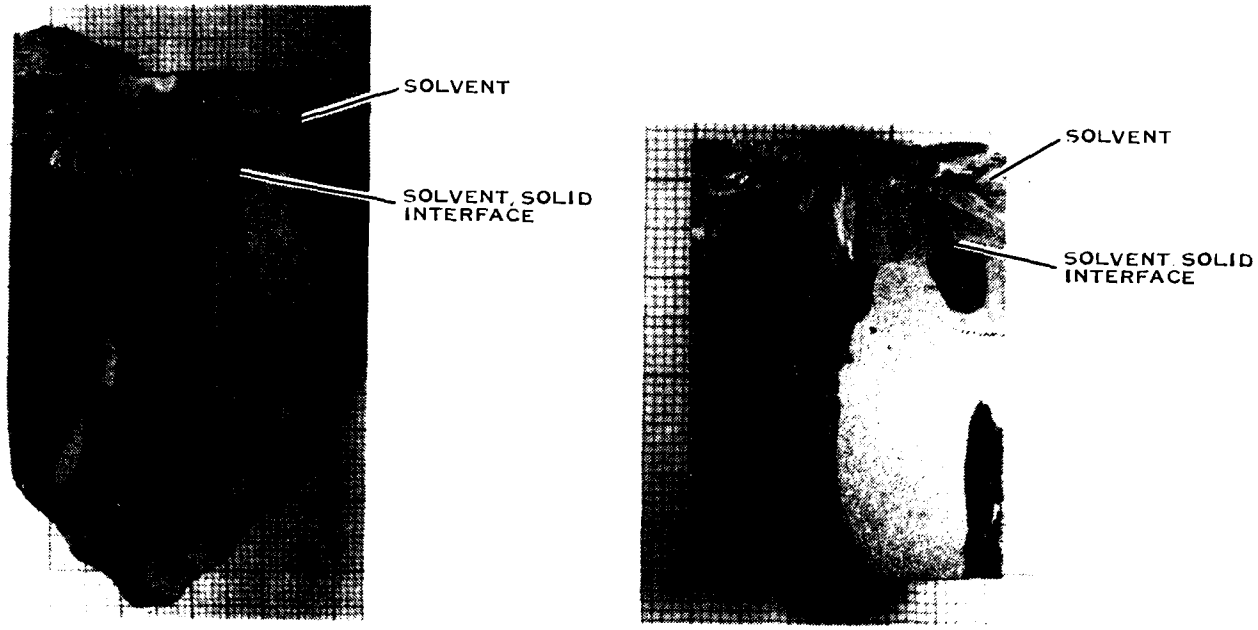

Figure 16. Macrostructure of (Hg,Cd)Te Ingots (Scale in mm)

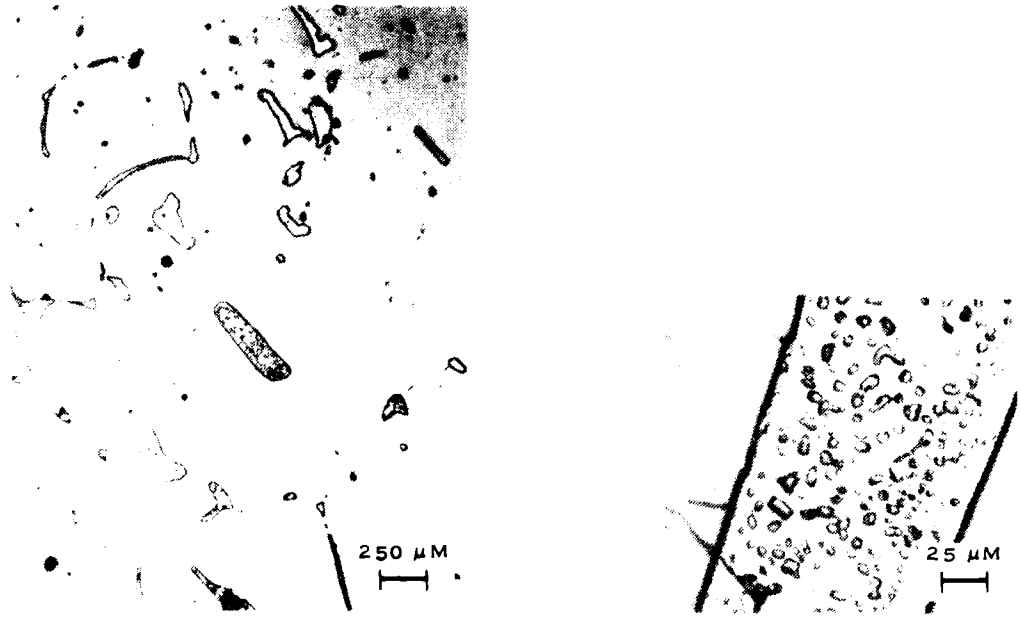

Figure 17. Microstructure of Ingots

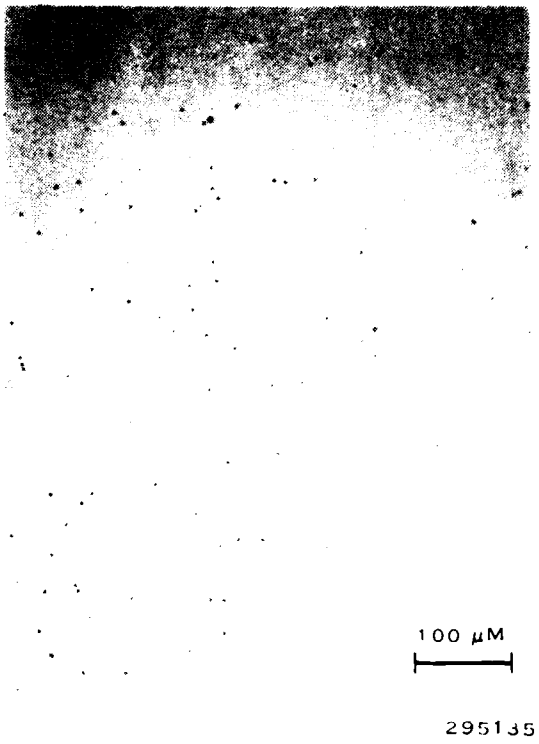

Figure 18. Microstructure of (Hg,Cd)Te Showing Dislocation Etch Pits Grown by THM Under a 120°C/cm Temperature Gradient

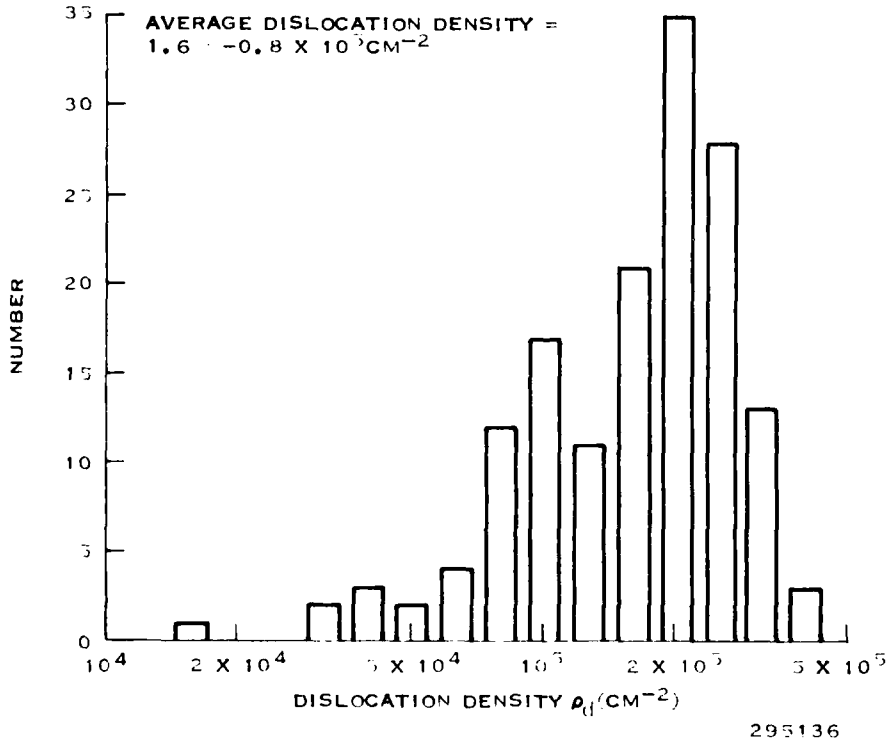

Figure 19. Dislocation Density Histogram Across a 40-mm-Diameter Wafer

SECTION IV

SUMMARY AND CONCLUSIONS

The objectives of this program were to examine the feasibility of using the incremental quenching technique to solidify homogeneous large diameter polycrystalline ingots and to grow large crystals by recrystallization and by the traveling heater method (THM).

Forty-mm-diameter (Hg,Cd)Te ingots weighing 700 grams have been solidified by the incremental quenching technique. The as-quenched ingots have been recrystallized to yield large diameter crystals (maximum 25-mm in diameter). The necessity of high pressure vessels to recrystallize the large ingots made it difficult to establish optimum growth conditions. The as-quenched ingots have been used as source material for crystal growth by THM. Unseeded growth runs have yielded large crystals (20 by 40 mm^2) with a dislocation density ranging from 5×10^4 to 3×10^5 cm^{-2}. The substructure density within the large grain is very low. In smaller crystals, 20 mm in diameter, grown by THM, the substructure density was almost completely removed except at the edges of the crystal. The dislocation density in these crystals ranged from 2×10^4 to 2×10^5 cm^{-2}. During this phase of the program, critical growth conditions for single-phase material were established as well as conditions giving rise to a minimum concavity of the growing interface away from the end of the ampoule. At the beginning of the growth, the interface is planar and its shape can be controlled by varying the ampoule and thermal conductivity. It was demonstrated that when incrementally quenched ingots are used, the dissolving interface is nearly flat.

The electrical properties of n-type (Hg,Cd)Te and (Hg,Cd,Zn)Te 20-mm-diameter crystals grown by THM indicate that purification during growth is achieved. The MIS device characteristics on n-type crystals indicate the dark currents generated within the material are diffusion limited and are within less than a factor of 10 of the Auger limit. The 40-mm-diameter crystals are presently being annealed for carrier-type conversion. For the results on the smaller crystals, it is expected that the larger crystals will have similar if not superior electrical and device characteristics.

APPENDIX A

GROWTH OF LARGE DIAMETER (Hg,Cd)Te CRYSTALS BY INCREMENTAL QUENCHING

Growth of large diameter (Hg,Cd)Te crystals by incremental quenching

Luigi Colombo, A. J. Syllaios, R. W. Perlaky, and M. J. Brau
Texas Instruments, Incorporated, Dallas, Texas 75266

(Received 1 June 1984; accepted 20 August 1984)

The growth of large (20 mm diam by 50 mm length) $Hg_{1-x}Cd_xTe$ crystals by incremental quenching of large volume $Hg_{1-x}Cd_xTe$ alloy melts was demonstrated. This method is based on the sequential freezing of shallow melts that have large surface to volume ratios onto a large diameter growing ingot. The resulting homogeneous polycrystalline ingots were annealed at 665 °C to promote grain growth. Grain sizes ranging from 25 to 35 mm were obtained after annealing at 665 °C for 28 days. In addition, the crystals showed very little substructure and had dislocation densities of $1.25 \pm 0.6 \times 10^5$ cm^{-2}. Hall effect measurements on wafers annealed at temperatures below 300 °C show an *n*-type behavior with carrier concentrations ranging from 3.3×10^{14} to 4.8×10^{14} cm^{-3} and majority carrier mobilities ranging from 1.69×10^5 to 2.29×10^5 cm^2/V s at 77 K for a composition $x = 0.225$. The compositional variation Δx in the radial and axial direction was measured by several techniques and was found to range from 0.005 to 0.01.

I. INTRODUCTION

Recently, there has been an increasing interest in large area (Hg,Cd)Te single crystals for large two dimensional infrared detector arrays. Growth of large area (Hg,Cd)Te crystals has been addressed by both thin film and bulk growth techniques. Thin film techniques such as liquid phase epitaxy, metal-organic chemical vapor deposition, and vapor phase epitaxy, while they provide large area and good lateral uniformity do not yet meet the stringent requirements of low line defect density, low carrier concentrations, and high minority carrier lifetime. Equilibrium bulk growth techniques, traditionally used for elemental semiconductors and binary compounds, are not suitable since these give rise to radial and axial composition variations which are a result of the large composition and vapor pressure dependent segregation coefficient of Cd with respect to Hg in (Hg,Cd)Te. In equilibrium growth techniques, it is generally found that the shape of the isocomposition surface corresponds closely to the shape of the melt solid interface.[1] In the case of diffusion controlled growth, homogeneous growth might be expected if the solidification front is planar. However, since the density of the (Hg,Cd)Te is composition dependent, convection dominates over diffusion, thus enhancing inhomogeneity.[2] Furthermore, heat flow considerations render the establishment of planar solidification fronts difficult. The current nonequilibrium bulk growth technique, specifically solid state recrystallization, although it provides crystals with low defect densities and high minority carrier lifetimes,[3] cannot provide the large areas required to fabricate large two dimensional infrared detector arrays. Triboulet *et al.*[4] at this conference have reported on the growth of 30 mm diam (Hg,Cd)Te using the traveling heater method utilizing a tellurium liquid zone. However, the technique suffers from the unavailability of homogeneous source material of the same diameter as the growing ingot.

The purpose of this paper is to report on a novel technique whereby the (Hg,Cd)Te melt is sequentially solidified onto a growing ingot in order to reduce compositional inhomogeneities in both the radial and axial directions. This technique will be referred to as incremental quenching.

The incremental quenching technique may be considered an extension of the previously mentioned solid-state recrystallization technique. Its global freezing character is, however, abandoned. Instead, this technique is based on sequential freezing of shallow melts with large surface-to-volume ratio that inherently have a small Biot number. Freezing occurs with minimal temperature gradients and in an essentially isobaric mode. Nonequilibrium freezing considerations indicate that the best approach to the rapid cooling of liquids is via heat transfer by conduction to a solid substrate. This is the basis of the "gun" and the "piston-and-anvil" quenching techniques.[5] In such techniques, the thickness of the liquid layer must be kept within certain limits and the freezing time must be short.[5] Consider a melt layer of volume V, density ρ, and base surface area S, initially at the liquidus temperature T_l, on a solid substrate of temperature T_0. The average heat rate generated during freezing is

$$Q_f = \rho V L / t_f, \tag{1}$$

where L is the latent heat of fusion and t_f is the time required for the melt layer to freeze. A lumped heat transfer formulation[6] yields the heat flow equation:

$$\rho C V dT/dt = Q_f - h(T - T_0)S, \tag{2}$$

where C is the melt heat capacity and h is the heat transfer coefficient to the solid substrate. Solution of differential Eq. (2) with the initial condition:

$$t = 0; \quad T = T_l \tag{3}$$

and the final condition:

$$t = t_f; \quad T = T_s \text{(solidus temperature)} \tag{4}$$

results in a transcendental equation for the freezing time:

$$t_f = \frac{\rho C}{h}\left(\frac{V}{S}\right) \ln\left[1 + \frac{T_l - T_s}{(T_s - T_0) - \frac{\rho L}{h}\left(\frac{V}{S}\right)\frac{1}{t_f}}\right]. \tag{5}$$

Therefore, short freezing times are obtained for thin layered melts where the volume-to-surface ratio is small.

J. Vac. Sci. Technol. A 3 (1), Jan/Feb 1985 0734-2101/85/010100-05$01.00

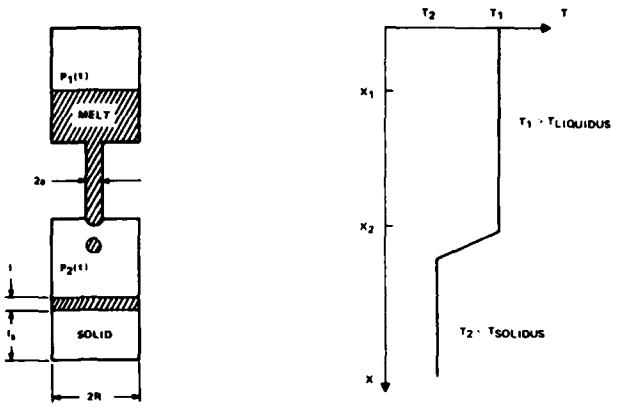

FIG. 1. Schematic diagram of the incremental quench process.

Based on these facts, an embodiment of incremental quenching is shown in Fig. 1. Small (Hg,Cd)Te melt drops are transferred to the lower chamber, spread over the top surface of the growing ingot, and solidify.

II. EXPERIMENTAL

The experimental apparatus used to quench 20 mm diam. ingots consists of a two-zone furnace utilizing two heat pipes separated by a 20 mm thick transite plate. (Hg,Cd)Te is prepared using high purity zone refined cadmium and tellurium and high purity mercury. After the appropriate quantities of Cd, Te, and Hg are weighed, they are placed in an hourglass shaped ampoule, evacuated and sealed. The ampoule is then placed in the furnace with the charge in the appropriate zone. The temperature of the furnace is then slowly increased to T_0 and T_l in such a way as to prevent material transport to the transfer chamber during the heating cycle. The material is kept at $T_l = 860$ °C for $x = 0.225$ for 2–3 h. The temperature of the melt is then decreased to $T_0 \sim 825$ °C and the furnace is rotated to transfer the melt. The temperature of the transfer zone, the orifice, and liquid are monitored using a chromel–alumel thermocouple with a data logger. After the melt is completely transferred the furnace is slowly cooled to room temperature. The ingot is then annealed at $T \sim 665$ °C for 4 weeks to achieve grain growth and compositional homogenization.

The as-quenched and recrystallized ingots are lapped using alumina powder and chemically polished using bromine methanol solutions to remove the saw and lapping damage. The surfaces are then etched to reveal etch pits delineating tellurium precipitates and dislocations using a Polisar 2 etchant[7] or a Texas Instruments proprietary etchant.

The wafers are then annealed at temperatures less than 300 °C to convert the as-grown p-type crystals to n-type. The carrier concentration and mobility of the crystals are measured at 77 and 300 K by the Hall effect.

The composition and compositional uniformity of the crystals was measured using four techniques: (1) infrared spectroscopy using Fourier transform spectrometer (FTIR), (2) electron probe microanalysis (EPMA), using energy dispersive spectrometry data acquisition,[8] (3) UV-visible reflectance (UV-VIS), and (4) photoconductive spectral cutoff wavelength.

III. RESULTS

A. (Hg,Cd)Te melt quenching

During the incremental quench process, the molten alloy is extruded through the orifice to form molten drops or a molten jet. The drops impinge on a solid substrate (or initially at the base of the ampoule) and are spread and solidified to form a growing ingot. One important condition that must be fulfilled for incremental solidification is

$$\frac{dl}{dt} < v_s, \tag{6}$$

i.e., the melt accumulation rate dl/dt must be smaller than the solidification rate v_s.

Figure 2(a) shows temperature variation of the solidification chamber during the liquid transfer. The temperature increases initially above T_0 (665 °C) and then decreases back

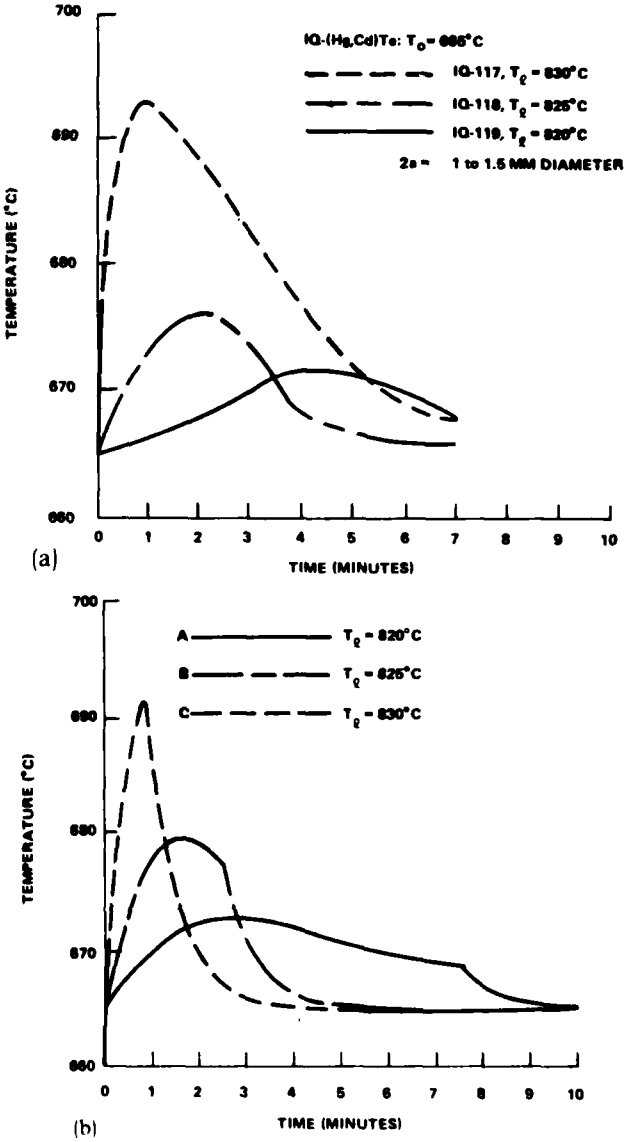

FIG. 2. (a) Time variation of the solidification chamber temperature as measured at the bottom of the ampoule during melt transfer and (b) calculated temperature variation of the solidified ingot during melt transfer.

to T_0. The temperature of the lower chamber during the liquid transfer did not exceed the solidus temperature and it decreased with the liquid temperature. A lumped analysis of this transient process is as follows. Consider melt drops of mass m and temperature T falling on the growing ingot and solidifying. Let m_0 be the initial mass of the ingot and heat-sink, C the heat capacity, L the heat of fusion of the $Hg_{1-x}Cd_xTe$ melt, and $\dot{M}$ is the rate of ingot mass increase. Then, neglecting for the moment heat transfer losses from the solidified ingot, the following thermal energy balance differential equation can be written:

$$[C\dot{M}(T_l - T) + \dot{M}L\,]dt = C(m_0 + \dot{M}t)dT \tag{7}$$

with initial conditions:

$$t = 0; \quad T = T_0. \tag{8}$$

Solution of Eq. (7) with the initial conditions of Eq. (8) yields:

$$T(t) = \frac{\dot{M}t\,[T_l + (L/C)] + m_0T_0}{m_0 + \dot{M}t} \quad 0 \leqslant t \leqslant t_f. \tag{9}$$

Differential Eq. (7) describes the temperature variation of the growing ingot during solidification. This equation holds when the heat losses from the ingot to the environment during solidification are ignored. If such losses are taken into account, the heating differential Eq. (7) is changed to:

$$[C\dot{M}(T_l - T) + \dot{M}L - \tilde{h}(A_0 + \dot{A}t)(T - T_0)]dt = C(m_0 + \dot{M}t)dT, \tag{10}$$

where A_0 is an effective area of the heatsink at the base of the solidification ampoule chamber and $\dot{A}$ is the rate of increase of the ingot area during solidification. After freezing (quenching) of the melt, the ingot temperature decays to the furnace temperature because of heat loss to the furnace. The following differential equation applies for $t > t_F$:

$$\tilde{h}A(T - T_0)dt = -(CM + C_0m_0)dT, \tag{11}$$

where $\tilde{h}$ is the heat transfer coefficient from the solidified ingot to the furnace through the fused silica ampoule, A is the heatsink surface area, and m_0 is the heatsink mass. The solution of differential Eq. (11) for $t > t_F$ is

$$T(t) = T_0 + [T(t_F) - T_0] \times \exp\left[-\frac{\tilde{h}A}{MC + m_0C_0}(t - t_F)\right]. \tag{12}$$

The heating Eq. (10), and cooling Eq. (11) describe the temperature variation of the solidified ingot during quenching. With the requirement that the temperature is a continuous function at the end of solidification, i.e., at time $t = t_F$, using the appropriate heatsink and material parameters $T(t)$ can be plotted as shown in Fig. 2(b), where for $t < t_f$, Eq. (10) is used and for $t > t_f$, the cooling Eq. (11) applies. Comparison of the calculated temperature variation during quenching with the experimental plots of Fig. 2(a) shows that this analysis is in qualitative agreement with the experimental results. A more comprehensive analysis of the temperature-time relationship during quenching should be based on a differential heat transfer formulation that takes into account the temperature gradients present in the ingot and the temperature variation of the thermophysical parameters of (Hg,Cd)Te.

Figure 3(a) shows the microstructure of an as-quenched ingot with an average grain size of approximately 225 μm; the grain size usually ranges from 50 to 500 μm. In addition the ingots contain a second phase (Hg,Cd)Te–Te eutectic at

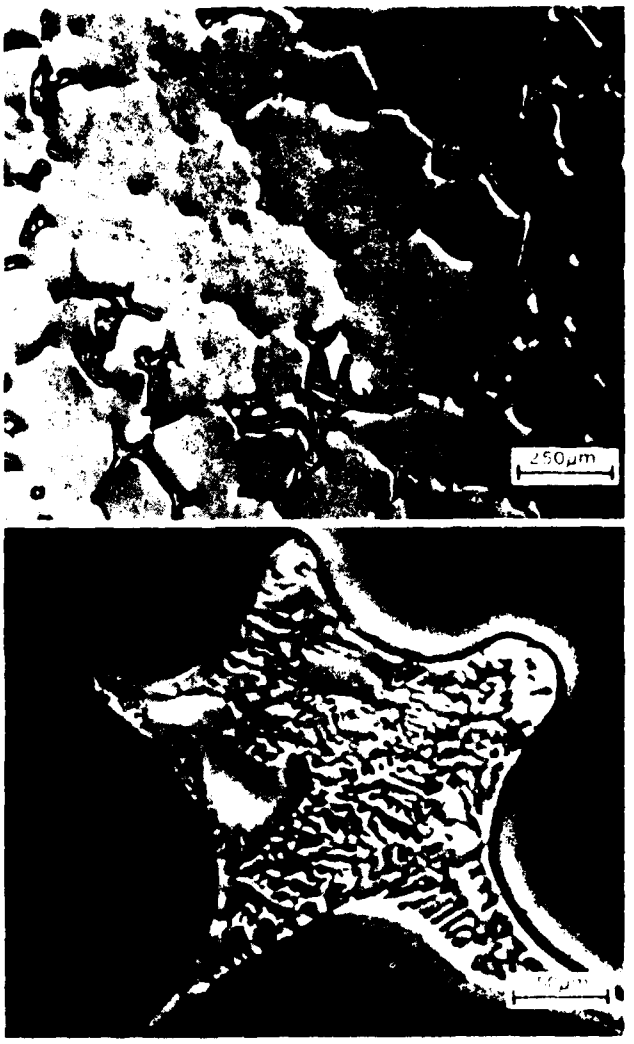

FIG. 3. Microstructure of an as quenched ingot (a) after bromine-methanol polish, (b) second phase (Hg,Cd)Te–Te eutectic at grain boundary.

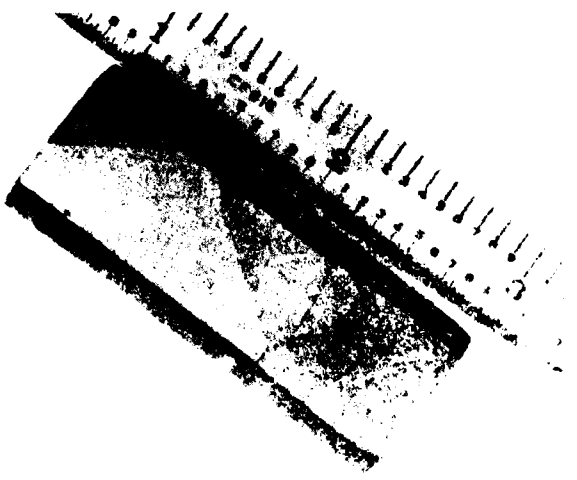

FIG. 4. Macrograph of an [illegible] heated at 600°C for 28 days.

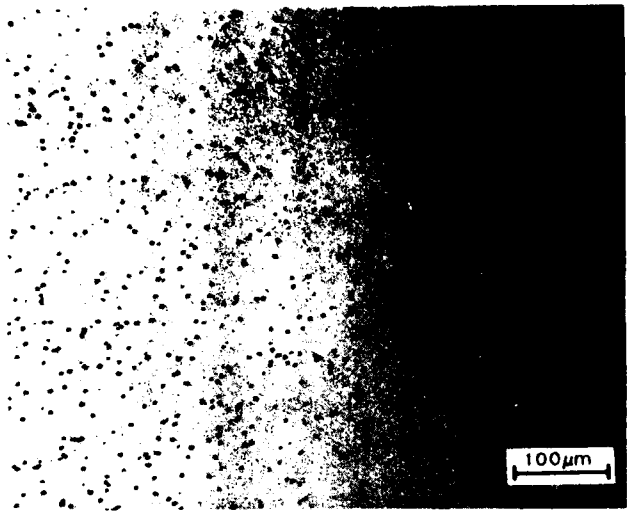

FIG. 5. Microstructure of incrementally quenched (Hg,Cd)Te annealed at 665 °C for 28 days under a mercury atmosphere.

the triple points as shown in Fig. 3(b). The dislocation density at the triple points is greater than 10^6 cm^{-2} indicating that the crystals are highly stressed. These regions evolve during annealing at 665 °C to yield a single phase material.

B. Grain growth

The grain size as a function of isothermal annealing time at 665 °C under a mercury vapor pressure shows the classical grain growth behavior with a time exponent n equal to 0.64. This value is slightly higher than the theoretical value of $\frac{1}{2}$. The higher exponent may be attributed to the fact that in most ingots an anomalous grain growth is observed. However, when the ingots are grown under Te-rich conditions, a Te-rich phase is observed at the grain boundaries and the anomalous grain growth is suppressed. This behavior has also been reported by Vere *et al.*[9]

Figure 4 shows the macrograph of an ingot annealed at 665 °C for 28 days. The crystals grown by this technique

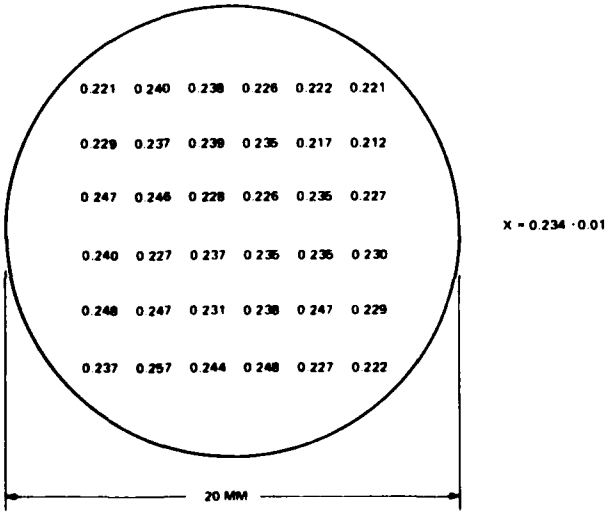

FIG. 6. Compositional uniformity in the radial direction as measured by electron probe microanalysis.

DISTANCE (MM)

DISTANCE (MM)	0	2	4	6	8
0	0.190	0.185	0.199	0.191	0.201
2	0.187	0.185	0.187	0.193	0.221
4	0.190	0.185	0.188	0.189	0.216
6	0.194	0.191	0.196	0.197	0.202
8	0.195	0.193	0.191	0.197	0.196
10	0.197	0.191	0.191	0.196	0.194
12	0.195	0.192	0.195	0.189	0.209
14	0.197	0.189	0.189	0.192	0.204
16	0.192	0.189	0.185	0.194	0.200
18	0.204	0.184	0.179	0.194	0.215

X = 0.194 ± 0.008

FIG. 7. Compositional uniformity in the axial direction as measured by electron probe microanalysis.

usually contain two to three grains. Figure 5 shows the microstructure of the ingot shown in Fig. 4. Clearly compositional homogenization has occurred, i.e., no second phase eutectic is present. The dislocation density as measured by the etch pit method is $1.25 \pm 0.6 \times 10^5$ cm^{-2} across the ingot. In addition, the crystals grown by this technique show very little substructure and in many crystals no substructure is observed.

C. Conductivity type conversion

The as-grown (Hg,Cd)Te crystals are p type due to the high group II vacancy concentration. In the case of high purity (Hg,Cd)Te the type conversion temperature would be much lower than 300 °C. The crystals grown in our laboratory, although high purity, still have a finite donor concentration and the type conversion temperature was typically around 270 °C.

The carrier concentration and mobility of wafers cut from the ingots and annealed at 270 °C for 2 weeks ranged from 3.3×10^{14} to 4.8×10^{14} cm^{-3} and 1.69×10^5–2.29×10^5 cm^2/V s for $x = 0.225$. The carrrier concentration and majority carrier mobility are comparable to those found in solid state recrystallized (Hg,Cd)Te.

D. Composition and compositional uniformity

The compositional uniformity of the crystals as measured by the various techniques with different spatial and composition resolutions varies from 0.005 to 0.01. The variation in Δx between the various techniques is attributed to the accuracy of the particular technique. Figures 6 and 7 show the compositional uniformity in the radial and axial direction of the ingot as measured by EPMA, respectively. Clearly the compositional uniformity as measured by the various techniques is in agreement with the initial premise that incremental quenching of the melt would give rise to a homogeneous solid.

IV. SUMMARY AND CONCLUSIONS

Growth of 20 mm diam. (Hg, Cd)Te crystals by incremental quenching of large melts has been demonstrated. The

quenched ingots with $x = 0.225$ annealed at 665 °C showed anomalous grain growth. The grain size ranged from 25 to 35 mm after annealing at 665 °C for 28 days. The crystals showed few subgrain boundaries and a dislocation density of $1.25 \pm 0.6 \times 10^5$ cm^{-2} as determined by the etch pit method. The compositional uniformity Δx as measured by the various techniques in both the radial and axial directions ranged from 0.005 to 0.01. This is in agreement with the initial premise that sequential freezing of the melt would give rise to a homogeneous ingot.

Hall effect measurements on wafers annealed at 270 °C for 2 weeks showed an n-type behavior with carrier concentrations ranging from 3.3×10^{14} to 4.8×10^{14} cm^{-3} and majority carrier mobility ranging from 1.69×10^5 to 2.29×10^5 cm^2/V s at 77 K for $x = 0.225$.

ACKNOWLEDGMENTS

The authors would like to thank Tom Moore for the EPMA measurements, Bill Breazeale for the photoconductor device fabrication and cutoff wavelength measurements, and Mark Bordelon for the infrared transmission measurements. This work is supported by DARPA through Contract No. MDA903-82-C-9439.

[1] R. Ueda, O. Ohisuki, K. Shinohara, and Y. Ueda, J. Crystal Growth **13/14**, 668 (1972).
[2] R. R. Galazka, T. Warminski, J. Bak, J. Auleytner, T. Dietl, A. S. Okhstin, R. P. Borovikova, and I. A. Zubritskij, J. Crystal Growth **53**, 397 (1981).
[3] M. J. Brau, L. Colombo, A. J. Syllaios, and M. J. Williams, *Status of Bulk (Hg,Cd)Te* (IRIS Materials Specialty Group, San Francisco, California 1984).
[4] R. Triboulet, T. Nguyen Duy, and A. Durand, J. Vac. Sci. Technol. A (these proceedings).
[5] P. Duwez, *Progress in Solid State Chemistry* (Pergamon, Oxford, 1966), Vol. 3, p. 377.
[6] For a lumped analysis of a plate, see for example, V. S. Arpaci, *Conduction Heat Transfer* (Addison-Wesley, Reading, Massachusetts, 1966), p. 76.
[7] E. L. Polisar, E. N. M. Boinikh, G. V. Indebaum, A. V. Vanyukov, and V. P. Schastlivii, Izv. Vyssh. Uchebn. Zaved. Fiz. **6**, 81 (1968).
[8] T. M. Moore, J. Vac. Sci. Technol. A **1**, 1651 (1983).
[9] A. W. Vere, B. W. Straughan, D. J. Williams, N. Shaw, A. Royle, J. S. Gough, and J. B. Mullin, J. Crystal Growth **59**, 121 (1982).

APPENDIX B

GROWTH OF 20-mm-DIAMETER (Hg,Cd)Te AND (Hg,Cd,Zn)Te BY THE TRAVELING HEATER METHOD

APPENDIX B

GROWTH OF 20-mm-DIAMETER (Hg,Cd)Te AND (Hg,Cd,Zn)Te BY THE TRAVELING HEATER METHOD

1. INTRODUCTION

Many bulk growth techniques have been used to grow (Hg,Cd)Te single crystals. Recently, Triboulet *et al.* have reported on the growth of compositionally uniform large diameter (Hg,Cd)Te by the traveling heater method (THM). One major shortcoming of their growth technique is the source material. Their source material is a composite of HgTe and CdTe in the appropriate proportions to yield the desired composition, x. In this form, the dissolving interface is inhomogeneous and can give rise to spurious growth. We have used incrementally quenched ingots as the source material to alleviate this problem. The objective of this program supported by IR&D funding was to demonstrate the growth of 20-mm-diameter oriented (Hg,Cd)Te single crystals at Texas Instruments, introduce zinc into the lattice to solid solution harden the crystal and determine the suitability of this material for focal plane array devices based on MIS technology.

Twenty-mm (Hg,Cd)Te and (Hg,Cd,Zn)Te single crystals oriented in the (111) direction have been grown by THM. The dislocation density varies from 2×10^4 cm^{-2} to 1×10^5 cm^{-2} as determined by chemical etching and the subgrain boundary density is very low in areas growing under flat or convex melt-solid interface shape. The material quality according to Hall effect measurements indicate that the material is undergoing purification and has a carrier concentration in the 1.6 to 2.2×10^{14} cm^{-3} range at 77 K at a magnetic field of 4 kG despite extensive material handling before growth. The MIS device characteristics also indicate that the material is diffusion limited at 77 K with dark currents of the order of microamps cm^{-2} for a spectral cutoff wavelength of 8.3 μm at 77 K.

2. RESULTS

a. Crystal Growth and Microstructure

The growth of (Hg,Cd)Te and (Hg,Cd,Zn)Te by THM has been carried out in a vertical geometry with a tellurium-rich solvent. The composition of the liquid allowed the use of the phase diagram data generated for liquid phase epitaxy. The growth temperature in our growth runs was kept at around 500°C. Figure B–1 shows schematically the ampoule with an appropriate seed, the solvent, and the source material. The source material, as in the case of 40-mm-diameter ingots and (Hg,Mn)Te, is an incrementally quenched ingot grown at the same conditions as the ingots grown during the first phase of the program described in Appendix A. Both CdTe and CdZnTe seeds used in this investigation were oriented in the ⟨111⟩ direction.

Figure B–2 shows the macrostructure of a crystal grown in the ⟨111⟩ direction both perpendicular to and parallel to the growth direction. We are currently growing on the A face. However, in view of the recent growth rate results of HgCdTe by molecular beam epitaxy (MBE) on the A and B face, crystals will be grown on the B face as well. There may be other significant advantages in growing on the fastest growing crystallographic orientation that are not evident at present. The interface shape away from the seed is concave and gives rise to formation of subgrain boundaries. Figure B–3 shows a series of micrographs taken along the ingot depicting the effect of interface shape on the microstructure. This is an important factor in evaluating the growth technique and prevailing growth conditions since these defects affect device performance. The dislocation density of these crystals ranges from 2×10^4 cm^{-2} to 1×10^5 cm^{-2} for an area of 20 by 40 mm^2 as shown by the histogram in Figure B–4.

The composition of the crystal was measured by electron microprobe analysis (EPMA), bandgap measurements at room temperature by Fourier transform spectroscopy, and by MIS device spectral cutoff wavelength at 77 K. Figure B–5 shows the compositional variation across a 20-mm wafer as measured by

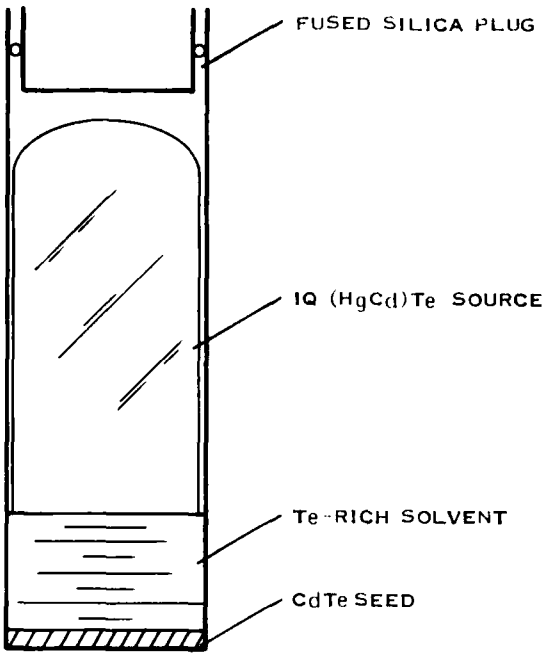

Figure B-1. Schematic Diagram of an Ampoule With Seed, Solvent, and Source Material

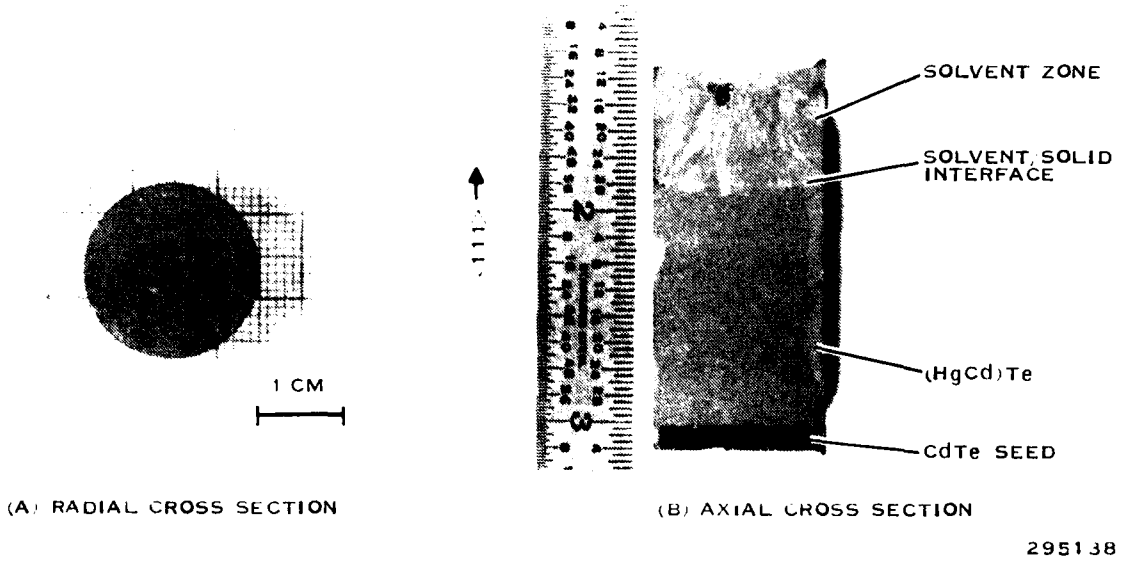

Figure B-2. Macrostructure of an Ingot Grown in the 111 Direction (Scale in mm)

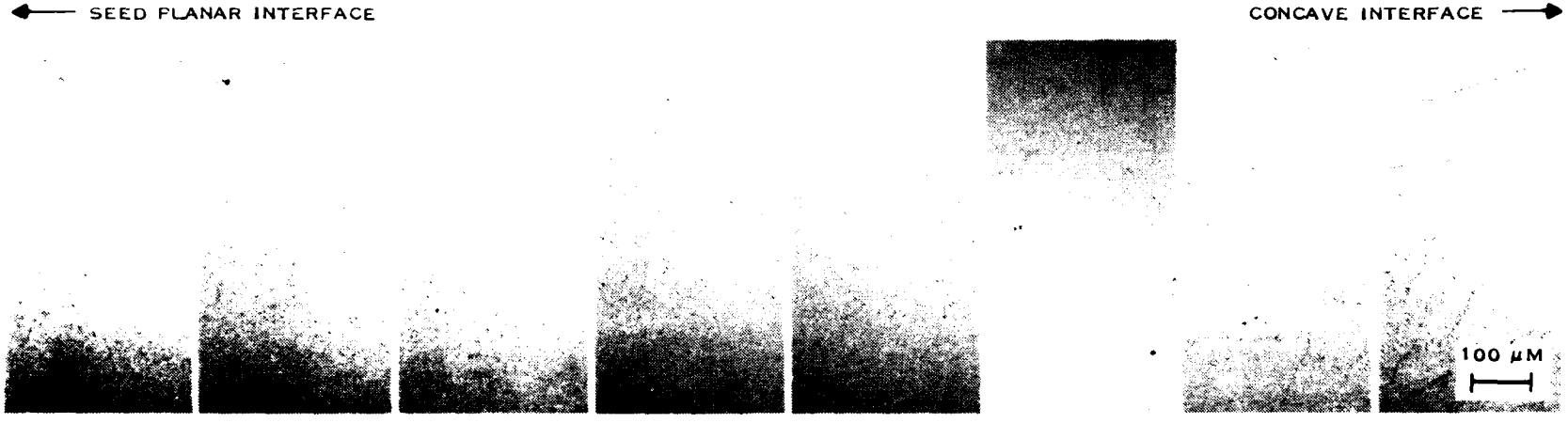

Figure B-3. Microstructure as a Function of Distance Along the Ingot Indicating the Onset of a Concave Interface Where the Subgrain Boundary Density is Higher

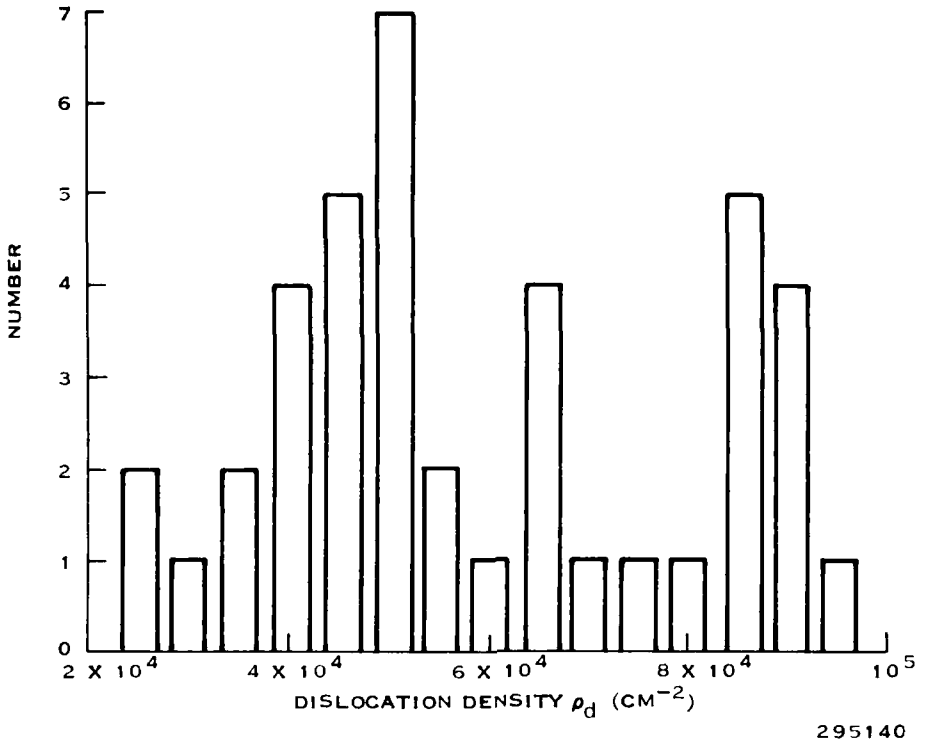

Figure B-4. Dislocation Density Histogram in a 20-mm Diameter (Hg,Cd,Zn)Te

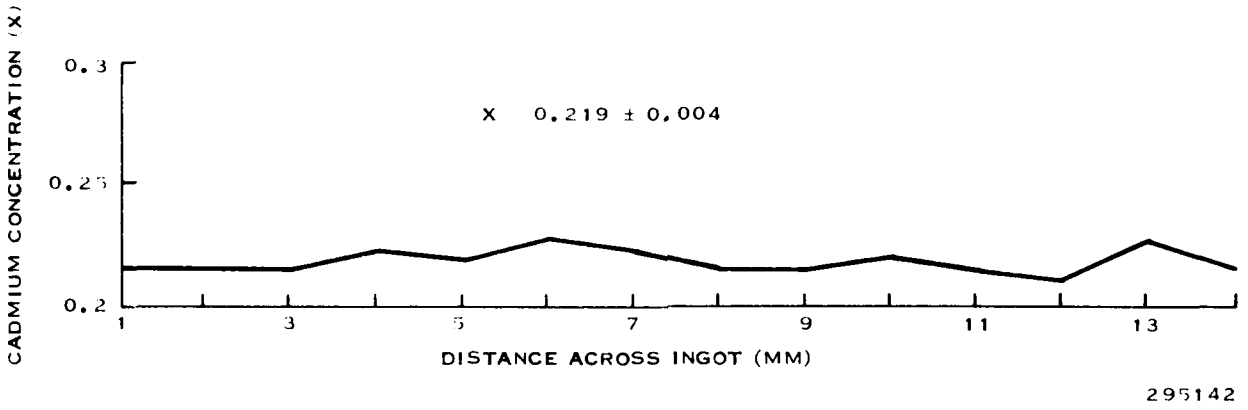

Figure B-5. Compositional Variation of (Hg,Cd)Te Grown at 500°C in the Radial Direction

TABLE B-1. COMPOSITIONAL UNIFORMITY OF CRYSTALS GROWN BY THM

Method	Composition	ΔX
EPMA	0.225	±0.004
FTIR (295 K)	0.23	±0.004
MIS Spectral (77 K)	0.244	±0.0013
	0.261	±0.004

EPMA. This is in agreement with the compositional variation as determined from room temperature bandgap measurements. Table B–1 shows a summary of the compositional variation as measured by the various techniques. The best samples have a compositional uniformity better than or equal to the best material grown by solid-state recrystallization.

b. Electrical and MIS Device Characteristics

Considerable attention has been paid to the electrical and device properties of any crystal grown since these will determine whether the technique is suitable for growth of useful material. The electrical properties were measured by the Hall effect at 77 K, room temperature, as a function of magnetic field and temperature on selected samples. Figure B–6 shows the carrier concentration of a crystal as a function of position in the growth direction. The carrier concentration measured at 4 kG is about 2×10^{14} cm^{-3} across the whole ingot. Comparable material grown by the solid-state recrystallization process has a carrier concentration a factor of 1.5 to 3 higher when using the same starting materials. This indicates that there is some degree of purification during this growth process. The temperature dependence of the transport properties shown in Figure B–7 also indicates that the material has reduced point defects. This behavior is in contrast to the anomalous transport properties often observed in (Hg,Cd)Te films grown by liquid phase epitaxy. The uniformity of the material is further affirmed by the magnetic field dependence of the Hall coefficient at all temperatures. Figure B–8 shows the magnetic field dependence of the Hall coefficient at 30 K and 80 K. It follows two carrier Chambers relation indicating high point defect and compositional uniformity. It is important to note that the mobility for this material is very high considering that the MIS spectral cutoff wavelength at 77 K is 7.5 μm with a corresponding composition $x = 0.251$.

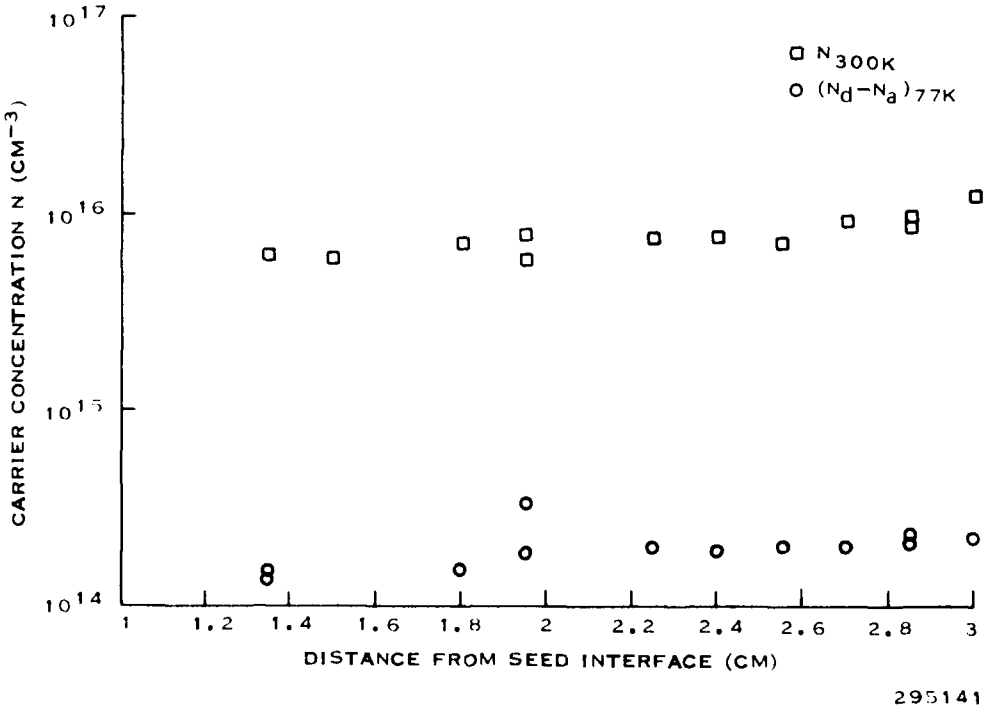

Figure B-6. Carrier Concentration as Measured by the Hall Effect at 77 K and 295 K Along the Ingot

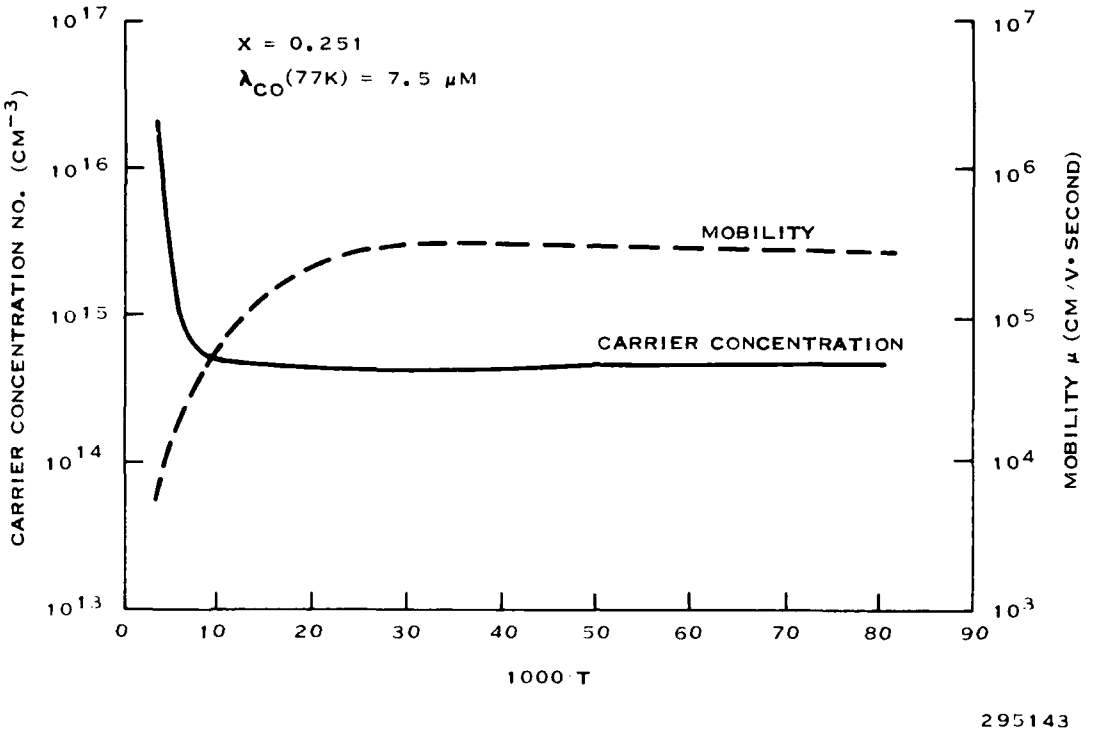

Figure B-7. Temperature Dependence of the Mobility and the Carrier Concentration for a Crystal With an L_{co} = 7.5 μm at 77 K

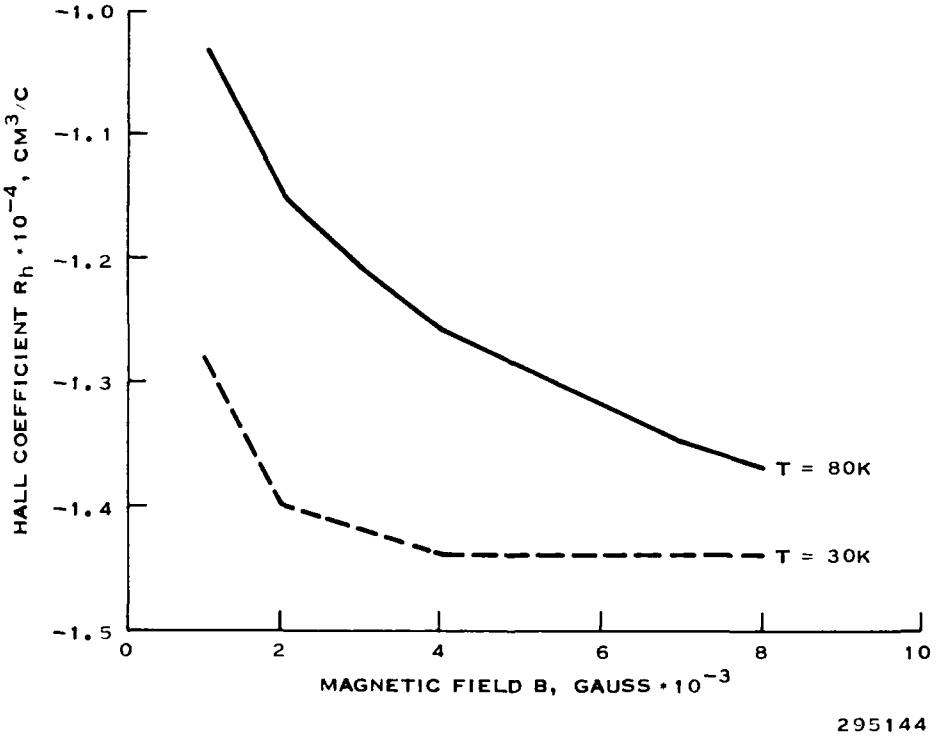

Figure B-8. Magnetic Field Dependence of the Hall Coefficient at 77 K and 30 K

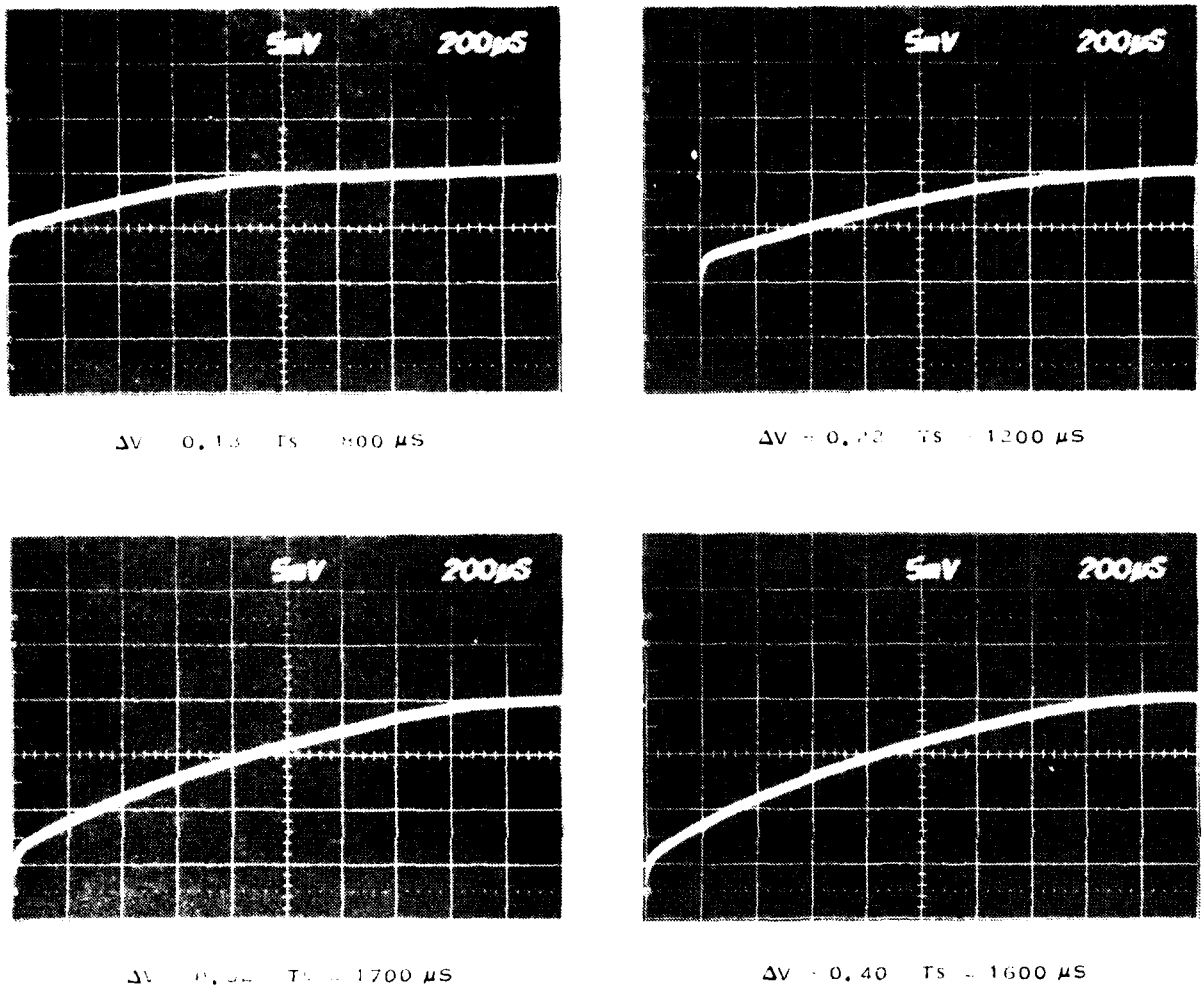

Figure B 9. MIS Device Decay Curves at 77 K Under Zero FOV as a Function of Bias Voltage (L_{co} = 8.3 μm at 77 k)

Metal insulator semiconductor (MIS) devices were fabricated on the crystals grown by THM using anodic oxide as the passivating layer and ZnS as the antireflection coating. The MIS device characteristics are listed in Table B–2 with a comparison of the carrier concentration measured by the Hall effect and from the C-V curves. The MIS device storage time is high and diffusion limited at 77 K. Figure B–9 shows the decay curves of the device as a function of bias voltage with a 77 K background (zero field of view). The dark current calculated from the MIS device storage time, although not directly comparable to material grown by solid-state recrystallization because of the wavelength shift, follows the same exponential behavior if plotted as a function of wavelength, as shown in Figure B–10.

3. SUMMARY

Oriented (Hg,Cd,Zn)Te single crystals have been grown by THM. The microstructure was correlated to the growing liquid-solid interface shape. Subgrain boundary free crystal structure was observed in areas where the crystal grew under flat or convex interface conditions. The dislocation density was also low.

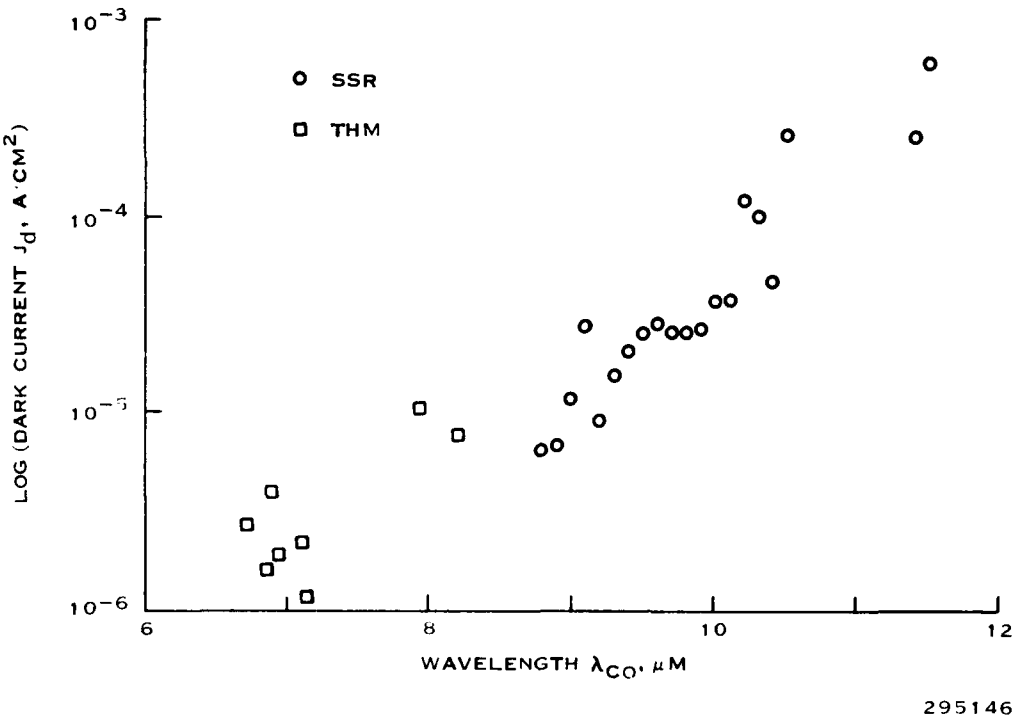

Figure B-10. Dark Current in (Hg,Cd,Zn)Te as a Function of Wavelength for Crystals Grown by the SSR Process and THM

TABLE B-2. TRANSPORT AND DEVICE PROPERTIES OF (Hg,Cd,Zn)Te GROWN BY THM

Sample No.	N(HALL-77 K) (cm^{-3})	N(MIS-77 K) (cm^{-3})	Mobility (77 K) ($cm^2/V \cdot sec$)	λ_{co} (μm)	Storage Time (ms)
THM-30-12	1.6×10^{14}	4.1×10^{14}	9.6×10^4	6.9	3.8
THM-30-13	1.9×10^{14}	3.8×10^{14}	9.8×10^4	6.7	5.8
THM-30-15	2.0×10^{14}	3.0×10^{14}	9.2×10^4	7.1	6.0
THM-30-16	1.9×10^{14}	4.1×10^{14}	9.1×10^4	6.9	6.2
THM-30-17	2.0×10^{14}	4.5×10^{14}	9.0×10^4	7.0	4.4
THM-30-18	2.0×10^{14}	3.8×10^{14}	1.17×10^5	7.2	12.0
THM-30-19	2.3×10^{14}	3.9×10^{14}	1.0×10^5	7.9	1.8
THM-30-20	2.2×10^{14}	4.3×10^{14}	1.19×10^5	8.3	2.2
THM-31-2	3.5×10^{14}	NM*	2.66×10^5	~12.0	NM
THM-31-4	3.8×10^{14}	NM	2.18×10^5	~12.0	NM

*NM = not measured

ranging from 2×10^4 cm^{-2} to 1×10^5 cm^{-2} for the majority of the crystals. Purification has been observed in these crystals. Electron mobilities of 1.19×10^5 $cm^2/V \cdot second$ have been observed and corresponding carrier concentrations of 2.3×10^{14} cm^{-3} at 77 K under a 4-kG magnetic field for $x = 0.24$. MIS devices built on these crystals showed uniform C-V characteristics with a diffusion limited behavior at 77 K under a 0-degree FOV. The carrier concentration measured from the C-V characteristics was in the range of 3 to 4.5×10^{14} cm^{-3} across the whole ingot. These results indicate that despite the extensive handling of the material before crystal growth, significant purification is achieved for impurities having small segregation coefficients. That is, all of the crystals grown so far have shown n-type behavior after low temperature annealing.

APPENDIX C

GROWTH OF (Hg,Mn)Te BY THE TRAVELING HEATER METHOD

APPENDIX C

GROWTH OF (Hg,Mn)Te BY THE TRAVELING HEATER METHOD

1. INTRODUCTION

Mercury manganese telluride [(Hg,Mn)Te] is an alternative infrared (IR) detector material for the 8- to 12-μm region. It is an attractive material because of its magnetic properties, i.e., one can magnetically tune the bandgap to improve the responsivity in the appropriate spectral region. The objective of this work is to evaluate this material as an IR detector and to compare it with (Hg,Cd)Te and (Hg,Cd,Zn)Te.

Several bulk growth techniques have been used so far to grow (Hg,Mn)Te crystals: Bridgman,[9] solid state recrystallization and incremental quenching,[10] and the traveling heater method (THM) discussed in this report. All four techniques have been investigated at Texas Instruments. Several problems have been encountered in the first three techniques. First, the material invariably reacted with the fused silica container wall; second, sticking together with the high oxygen concentration led to poor macrostructure because of grain boundary pinning by oxide particles. Manganese oxide inclusions observed within the grain usually showed high dislocation density in the vicinity. The Bridgman technique also gives rise to high compositional inhomogeneities.

To date, there has been very little work on the growth of homogeneous (Hg,Mn)Te by bulk techniques. The large segregation coefficient of Hg and Mn in the melt prevents most bulk techniques from being suitable for the growth of uniform crystals. Epitaxial techniques have been reported as giving rise to good quality material with photovoltaic performance comparable to that of (Hg,Cd)Te. However, these results are more a function of the process rather than the intrinsic property of the material. We have chosen THM to grow bulk crystals. This technique is basically a continuous liquid phase epitaxy technique with the advantages of purification and controlled equilibrium growth. Also, high compositional uniformity can be achieved in the radial and longitudinal directions. This technique is superior to LPE because it allows one to purify the material further during growth and to control the point defect concentration and line defect concentration by appropriate annealing procedures.

2. EXPERIMENTAL

The furnace used to grow (Hg,Mn)Te is shown in Figure 12 of the report. It is a three-zone furnace with a resistive central heater and two-post heaters to control the temperature gradient and the zone width. Growth by THM requires a seed, a solvent zone, and an (Hg,Mn)Te source. The starting materials used are 99.9999-percent tellurium from Cominco, Inc., 99.999999-percent mercury from Bethlehem and 99.99-percent puratronic grade manganese from Johnson Matthey. The solvent material is first reacted and cut into an appropriate length to match the width of the zone and then placed on top of the CdTe seed. The source material is made by the incremental quenching technique. The ingot is usually 50 to 60 mm long and 20 mm in diameter. This ingot is placed on top of the solvent in the fused silica ampoule, evacuated, and sealed. The growth rate used ranges from 2 to 3 mm/day at a growth temperature of 500°C.

3. RESULTS

a. Crystal Growth and Microstructure

Two critical conditions must be satisfied to grow low dislocation and subgrain-boundary density-oriented single crystals. The first is partial seed dissolution to ensure seeding and, therefore, single-crystal growth at the beginning of the growth. Second, the thermal losses during growth must be such that the growing interface is either flat or convex. The seed dissolution was accomplished by very careful temperature and ampoule position control during the initial stage of the growth without completely dissolving the seed or not dissolving it at all.

The melt-solid interface shape greatly influences the macrostructure and the microstructure of the growing crystal. Thermal management is, therefore, extremely important. Furnace design and ampoule design are of utmost importance. For example, self-seeding geometries (preferred in the initial stages of the program to save time and seeds) are inappropriate because of heat losses at an angle with respect to the growth axis. These give rise to a highly concave interface and self-seeding is forfeited. Figure C-1 shows the initial growth interface when a pointed ampoule is used. Also, the low thermal conductivity of the growing crystal causes the interface to be dominated by radial thermal losses rather than axial losses through the solid as the crystal grows. A more desirable ampoule shape is one with a flat end since this gives rise to an initial flat growing interface. Figure C-2 shows the interface radius of curvature as a function of position along the ingot. Clearly, as the ingot grows the interface reaches an equilibrium concave shape. However, in some cases, single-crystal growth continues but the microstructure begins to show subgrain boundaries.

Figure C-3 shows a micrograph of the CdTe seed (Hg,Mn)Te interface. The dislocation density at the interface is high, greater than 1×10^8 cm^{-2}; it cannot be measured by chemical etching techniques. These seeds were not lattice matched to (Hg,Mn)Te because of the difficulty in composition control at the beginning of the growth. Also, since the material near the seed interface is not used, it turns out that lattice matching is not important. Also notice the propagation of the twin to the ingot from the substrate. Although this is not desirable in this case, it shows epitaxial growth clearly. The dislocation density of the crystal as a function of position in the axial direction is shown in Figure C-4. This is typical of the ingots and similar to films grown by liquid phase epitaxy. Tellurium precipitates have not been observed in the as-grown crystals as determined by chemical etching.

The compositional variation was measured by Electron Microprobe Analysis along and across the wafer. Under the prevailing growth conditions of 3 mm/day and a solidification temperature of 500°C, the compositional variation across the ingot for $x = 0.12$ is ± 0.004. At the beginning of the growth, dislocation walls are sometimes observed along the solidifying interface outlining the interface shape. This is attributed to compositional variations as a result of poor local temperature control and possible re-dissolution of the growing crystal. These can also arise from periodic impurity incorporation and a combination of temperature oscillation and impurity incorporation as observed with Czochralski grown crystals.[6]

The compositional homogeneity has also been evaluated by room temperature carrier concentration measurements of wafers cut in the radial direction. The variation of the carrier concentration measured at room temperature is shown in Figure C-5. Initially, there is a slight transient region caused by temperature inaccuracies that occur since the moving ampoule system causes thermal profile variations. At the end of the ingot, a second transient is observed. This is attributed to the complete source dissolution. That is, the condition

$$C_o \rightarrow \frac{C_o}{k} \rightarrow C_o$$

is not satisfied, where C_o is the feed composition and the growing crystal composition and k is the segregation coefficient of either Hg or Mn. At the center of the ingot a steady-state region is achieved. The exact thermal conditions to achieve steady state from the beginning of the growth can be optimized to occur only a few micrometers from the seed interface as in the case of the traditional LPE growth.

c. Electrical and Device Properties

The electrical properties of the crystals have been assessed by Hall effect measurements at room temperature and liquid nitrogen temperatures and as a function of temperature on selected samples. Figure C-5 shows the room temperature carrier concentration as a function of position along the ingot in the growth direction. The ingot is initially Mn rich and slowly levels off, reaching a plateau, and then it decreases as the Mn is depleted from the melt as a result of complete source dissolution. This behavior

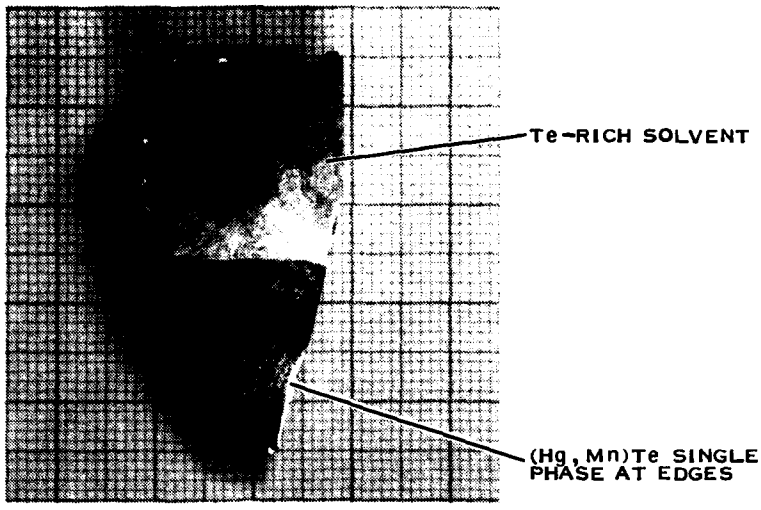

Figure C-1. Initial Growth Interface of (Hg,Mn)Te Grown in a Pointed Ampoule by THM (Scale in mm)

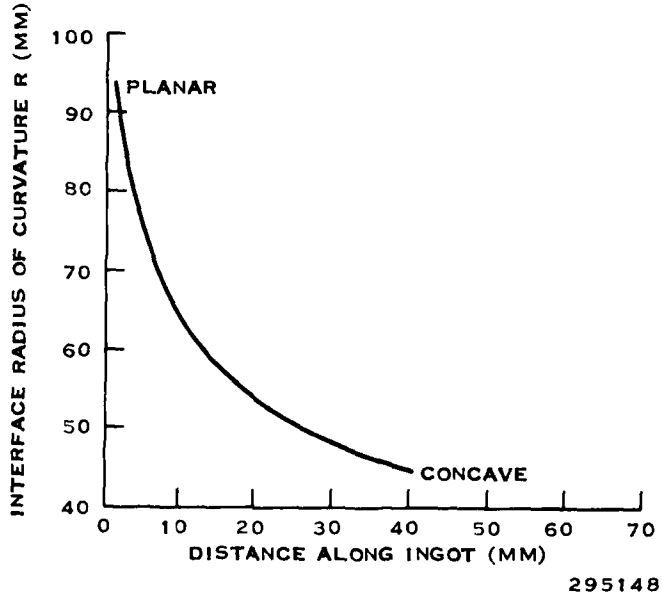

Figure C-2. Interface Radius of Curvature as a Function of Position Along the Ingot for a Flat-Bottom Ampoule

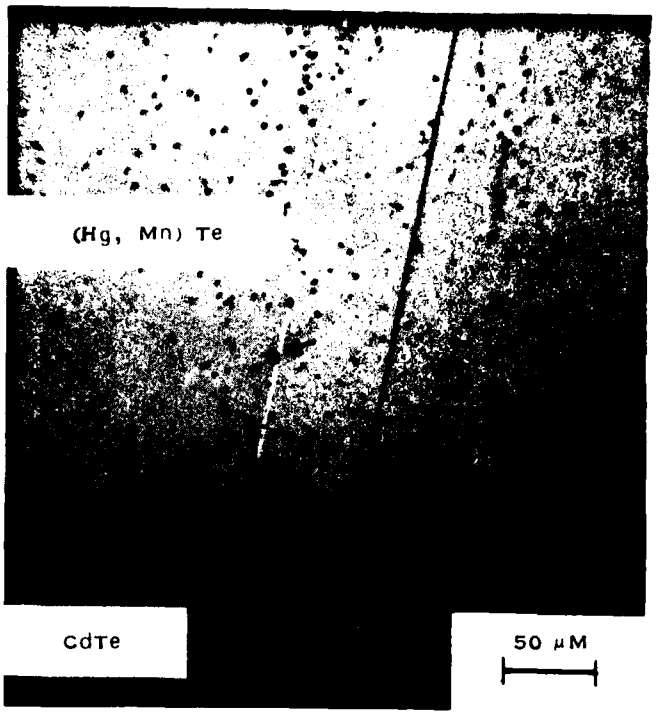

Figure C-3. Micrograph of a CdTe/(Hg,Mn)Te Interface Showing a High Interfacial Dislocation Density and a Propagated Twin

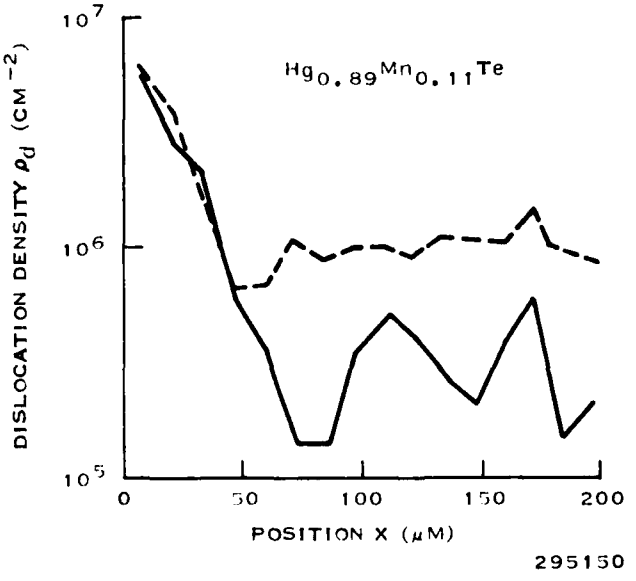

Figure C-4. Dislocation Density as a Function of Position Away From the CdTe Seed Interface as Revealed by Chemical Etching

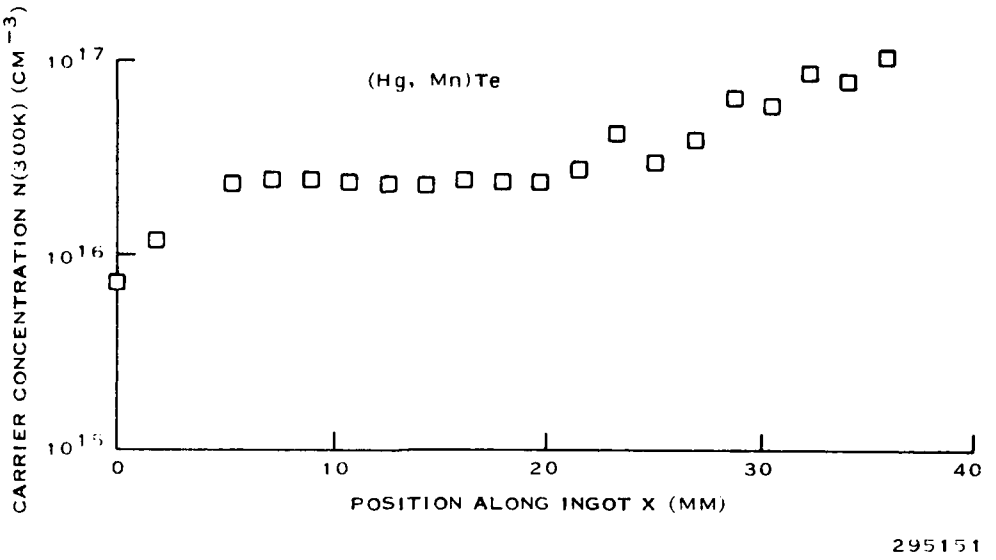

Figure C-5. Room Temperature Carrier Concentration as a Function of Position Along the Ingot

has also been observed in (Hg,Cd)Te. The temperature dependence of the mobility and the carrier concentration shows classical behavior with a mobility peak at 30K of 1.73×10^5 cm^2/V-second as shown in Figure C-6. The magnetic field dependence of the Hall coefficient also shows that the material follows a classical two-carrier-model Chambers relation indicating compositional and point defect structure homogeneity.

Both photoconductive and metal insulator devices have been built on the crystals. The photoconductive devices showed detectivities as high as 3.2×10^9 cm Hz$^{0.5}$/W and a responsivity of 7.4×10^4 V/W at 77 K for a $\lambda_{co} = 11.3$ μm as shown Table C-1.

4. SUMMARY AND CONCLUSIONS

The THM was used to grow compositionally uniform (Hg,Mn)Te oriented single crystals. The technique has demonstrated the potential of purification during growth. This is especially useful in this case since manganese is not available in high purity and purification of elemental manganese can be time-consuming. Dislocation densities ranging from 8×10^4 cm^{-2} to 3×10^5 cm^{-2} have been achieved and large areas of subgrain boundary free material have been obtained by carefully controlling the melt/solid interface shape. Carrier concentrations of 3.3×10^{14} cm^{-3} and mobilities of 7.5×10^4 cm^2/V-second at 77 K have been measured by the Hall effect for material with a room temperature carrier concentration of 2.2×10^{16} cm^{-3}. The crystals grown by the THM so far have shown superior transport properties in comparison with (Hg,Mn)Te grown by the solid-state recrystallization process. Photoconductive devices have been built on these crystals for the first time and have shown detectivities of 3.1×10^9 cm Hz$^{0.5}$/second and responsivities of 7.4×10^4 V/W for a λ_{co} of 11.4 μm under a 500 K background with a 180-degree field of view. Although the device performance is about a factor of 10 lower than devices on (Hg,Cd)Te, the performance can be improved with further material purification.

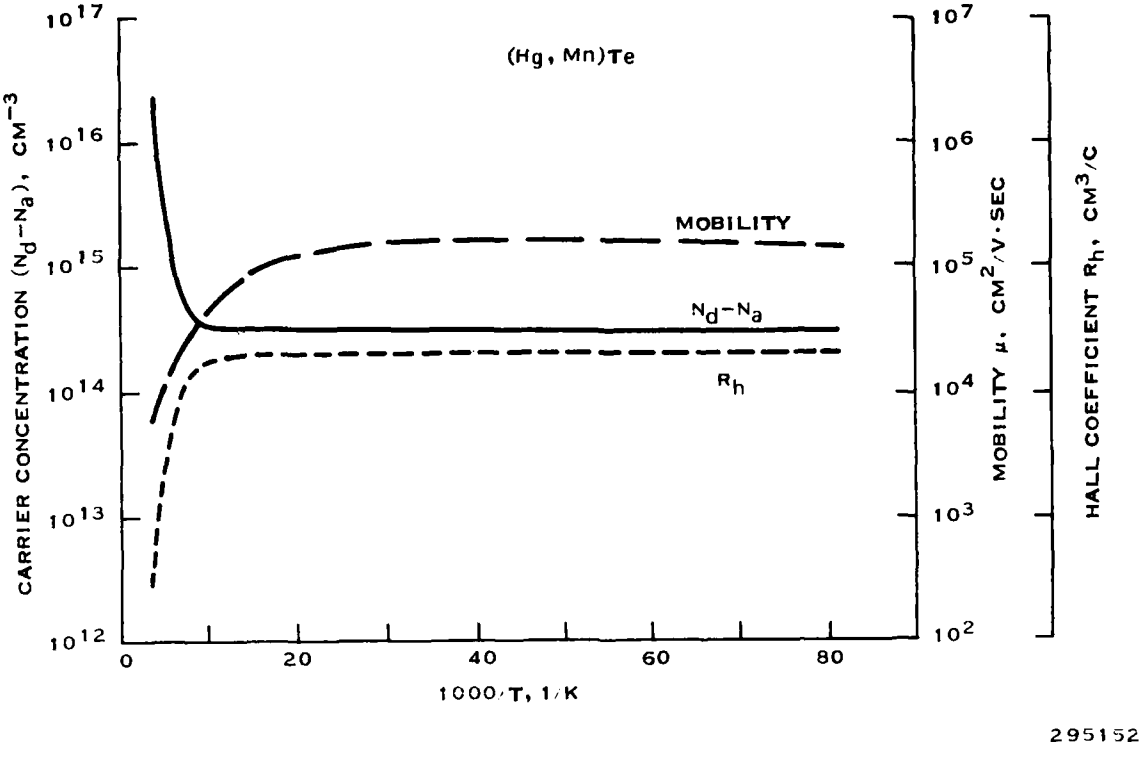

Figure C-6. Temperature Dependence of the Mobility and Carrier Concentration of (Hg,Mn)Te at 4 kgauss

TABLE C-1. PHOTOCONDUCTIVE CHARACTERISTICS OF (Hg,Mn)Te WITH 500K BACKGROUND AND 180-DEGREE FOV

Slice No.	I (mA)	D* (10^9 cm $Hz^{0.5}$/W)	R (V/W)	λ_{co} (μm)
MMT-11-2	1	2.36	12,872	
	2	2.46	24,740	
	3	3.19	57,724	11.1
	4	3.08	74,217	
MMT-11-1	2	2.28	11,911	
	3	2.07	18,325	11.3
	4	1.47	26,571	

REFERENCES

1. G.A. Wolff, "Travelling Solvent Techniques" in *Crystal Growth Theory and Techniques*, Ed. C.H.L. Goodman [Plenum Press: London (1974)], p. 193.
2. J.L. Lehoczky and F.R. Szofran in: *Materials Processing in the Reduced Gravity Environment of Space*, Ed. G.E. Rindone [North-Holland: Amsterdam (1982)], p. 409.
3. L. Colombo, U.S. Patent No. 4,582,683 (1986).
4. L.Colombo, "Growth and Characterization of (Hg,Cd,Zn)Te," *Proceedings of the IRIS Detector Specialty Group Meeting*, Seattle, WA (August 1984).
5. R. Triboulet, T. Nguyen Duy and A. Durand, "THM a Breakthrough in $Hg_{1-x}Cd_xTe$ Metallurgy," *J. Vac. Sci. Technol* **A-3** (1985), pp. 95–99.
6. E. Kuroda, H. Kozuka, and Y. Takano, *J. Cryst. Growth* **68** (1984), pp. 613–623.
7. P. Becla, "IR PV Detectors Utilizing HgMnTe and HgCdMnTe Semimagnetic Alloys," Extended Abstracts, The 1985 U.S. Workshop on the Physics and Chemistry of Mercury Cadmium Telluride, October 8–10, 1985, San Diego CA.
8. F.P. Incropera and D.P. DeWitt, *Introduction to Heat Transfer* [John Wiley & Sons (1983)].
9. R.T. Delves, *Br. J. Appl. Phys.* **16** (1965), p. 343.
10. L. Colombo, unpublished data.

END

DTIC

7-86